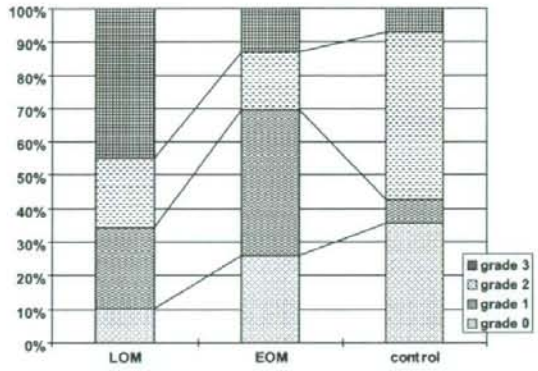

Fig. 2. The distribution of Fazekas DWMH ratings in LOM, EOM, and control groups. *Note.* LOM, late-onset mood disorder group; EOM, early-onset mood disorder group.

$P = 0.015$), FL ($F = 3.29$, df = 2, $P = 0.044$), and POL ($F = 6.35$, df = 2, $P = 0.003$). In the post hoc tests between LOM and EOM, significant differences were detected in FR ($P = 0.033$), FL ($P = 0.043$), and POL ($P = 0.003$). Between LOM and EC, a significant difference was detected in FR ($P = 0.048$).

3.2. Linear multiple regression analysis using the DWMH ratings as dependent variable

Results of linear multiple regression analysis are shown in Table 4. We obtained a significant regression model to predict the DWMH ratings ($F = 16.5$, $P < 0.001$); age, number of ECTs, and LOM were selected as significant variables ($t = 5.5$, -3.7, and 2.5; $P < 0.001$, 0.01, and 0.05, respectively).

4. Discussion

This study is unique in that we compared white matter lesions with regard to brain areas among the age- and gender-matched LOM, EOM and EC groups that include major depressive disorder and bipolar disorder. As for DWMH, LOM exhibited a higher rating than EOM; as for brain areas, significant between-group differences were detected in bilateral frontal areas and in the left parieto-occipital area. LOM, but not EOM, tended to show more severe pathological changes than the EC group, and there was a significant difference in the severity of changes in the right frontal areas. As for PVH, there was no difference among the three groups. In the linear multiple regression

Table 3
Fazekas ratings and *P*-values for comparison among late-onset mood disorder ($n = 29$), early-onset mood disorder ($n = 23$), and elderly control ($n = 14$) groups

	LOM	EOM	Controls	One-way ANOVA		Post hoc test *P*-value (Tukey HSD)		
				F-value	*P*-value	LOM vs. EOM	LOM vs. controls	EOM vs. controls
DWMH, mean (SD)	2.00 (1.07)	1.17 (0.98)	1.29 (1.07)	4.67	0.013	0.016*	0.096	0.946
PVH, mean (SD)	1.28 (1.22)	0.61 (1.08)	0.71 (1.14)	2.43	0.096	0.105	0.301	0.961
FR, mean (SD)	1.76 (1.18)	1.00 (1.00)	0.93 (0.83)	4.52	0.015	0.033*	0.048*	0.978
FL, mean (SD)	1.72 (1.19)	0.96 (1.07)	1.14 (1.03)	3.29	0.044	0.043*	0.253	0.875
POR, mean (SD)	1.14 (1.06)	0.48 (0.85)	0.86 (0.86)	3.09	0.052	0.041	0.637	0.472
POL, mean (SD)	1.31 (1.07)	0.43 (0.79)	0.64 (0.74)	6.35	0.003	0.003*	0.073	0.782
TR, mean (SD)	0.83 (1.00)	0.48 (0.90)	0.50 (0.52)	1.21	0.305	0.340	0.495	0.997
TL, mean (SD)	0.86 (1.03)	0.57 (0.95)	0.64 (0.63)	0.75	0.498	0.490	0.749	0.967
BGR, mean (SD)	0.62 (0.86)	0.43 (0.79)	0.29 (0.47)	0.97	0.385	0.664	0.380	0.836
BGL, mean (SD)	0.66 (0.97)	0.43 (0.84)	0.21 (0.43)	1.36	0.264	0.618	0.249	0.721

Note. LOM, late-onset mood disorder group; EOM, early-onset mood disorder group; DWMH, deep white matter hyperintensity; PVH, periventricular hyperintensity; FR, right frontal area; FL, left frontal area; POR, right parieto-occipital area; POL, left parieto-occipital area; TR, right temporal area; TL, left temporal area; BGR, right basal ganglia; BGL, left basal ganglia.
* One-way ANOVA $P < 0.05$ and post hoc test $P < 0.05$.

Table 4
Prediction of the DWMH ratings

	Dependent valiable	Variables entered	Standardized coefficients	*t*	R^2	*F*
$n = 52$	DWMH ratings				0.52	16.5***
df (1,44)		Age	0.61	5.5***		
		number of ECTs	−0.40	−3.7**		
		LOM group	0.27	2.5*		

Note. Multiple linear regression, stepwise method, DWMH: deep white matter hyperintensities, ECT: electro convulsive therapy, LOM: late-onset mood disorder.
* $P < 0.05$.
** $P < 0.01$.
*** $P < 0.001$.

analysis using the DWMH ratings as dependent variable, age, number of ECTs and LOM were observed as significant independent variables. The observation that about 80% of patients examined in the present study suffered from major depressive disorder suggests that the findings in this study largely reflect the factors associated with major depressive disorder.

There are many reports that DWMHs are more severe in late-onset depression than in normal controls (Greenwald et al., 1996; Kumar et al., 1997; Tupler et al., 2002), which agrees with our results. As for PVH, we found no significant difference between the mood disorders and the control subjects, which also agrees with many previous studies (Greenwald et al., 1996; Lenze et al., 1999; Tupler et al., 2002). However, some previous studies showed that there is a difference (Coffey et al., 1993; Kumar et al., 1997; Iidaka et al., 1996). Discrepancies between studies may be due to differences in sample size, chronological age of subjects, or other sampling characteristics.

Few studies have made a comparison between late-onset and early-onset depression patients of the same generation. Fujikawa et al. (1993) compared between the late and early-onset depression groups, reporting that the late-onset depression group has a higher rate of white matter lesions than the early-onset depression group. Salloway et al. (1996) reported that DWMH as well as PVH were significantly more severe in the late-onset depression group than in the early-onset depression group. Greenwald et al. (1996) reported that elderly depressed patients manifested significantly more severe hyperintensity ratings in the subcortical gray matter than age-matched controls, but between the early and late-onset groups whose age and cerebrovascular disease risk were identical, both DWMH and PVH showed no differences. However, Tupler et al. (2002) reported that although there was some difference in age between the groups, DWMHs were more severe with the late-onset than in the early-onset patients and controls, whereas no difference was noted for PVH. Among these reports, our results agree most closely with those of Tupler et al. (2002).

There were even fewer studies that compared between age-matched early- and late-onset groups with regard to brain areas. In our present study, LOM showed significantly more severe white matter lesions in the bilateral frontal areas and the left parieto-occipital area than did EOM. Tupler et al. (2002) reported that the lesions in the left middle and posterior areas correlated with their late-onset group, which agrees with our results. However, Tupler et al. (2002) also reported that there was no difference in the severity of white matter lesions in either frontal lobe areas between the late- and early-onset groups. Although they did not classify their patients according to age at onset, Taylor et al. (2003) reported that in the depression group, the severity of white matter lesions in the bilateral frontal areas and the left middle area correlated with age and that, in normal controls, the severity of white matter lesions in bilateral middle areas, but not in any frontal areas, showed the same correlation, as shown by statistical parametric mapping. The topographical pattern shown in their depression group is close to that in our LOD group, who showed more severe pathological changes than EOD and EC in similar brain regions. We consider it as a merit that Fazekas scale is easily applicable to daily clinical settings. However, Fazekas scale is more coarse tools to quantify the high intensity lesions than modern neuroimaging programs that generate volumetric data. This point is the limitation of the present study.

As for the frontal lobe in depressed patients, there have been several studies indicating differences from controls, such as volume decrease (Coffey et al., 1993; Kumar et al., 1998), glucose metabolism deterioration determined by positron emission tomography (PET) (Videbech, 2000; Drevets, 2001), aberration in phospholipid or energy metabolism in magnetic resonance spectroscopy (MRS) (Kumar et al., 2002), and cognitive dysfunction determined by neuropsychological studies (Fossati et al., 2002). The frontal lobes have mutual fiber communications with the subcortical nuclei, such as the thalamus, basal ganglia, and the amygdaloid body, with five independent parallel circuits proven, which Tekin and Cummings (2002) organized and classified into two groups: (1) the dorsolateral prefrontal and lateral orbitofrontal subcortical circuits and (2) the medial orbitofrontal and anterior cingulate circuits. Projections from the mesencephalon or the subcortical gray matter to the frontal lobes are related to the emotional processing of information and the maintenance of emotional state, and some investigators postulate that these neural networks may be disturbed in depression (Brody et al., 2001). Therefore, it is possible that functional deficits in the frontal lobes are caused by subcortical lesions within these circuits, resulting in secondary functional deficits in the frontal areas that trigger mood disorders.

As for the percentage of patients with medical comorbidities, such as diabetes, hypertension, hyperlipemia, ischemic heart disease, cardiac arrhythmia, habitual alcohol drinking and habitual smoking, that are risk factors for cerebrovascular lesions, there was no difference between LOM and EOM. In addition, such factors were not selected as significant variables in the linear multiple regression analysis using the DWMH ratings as dependent variable. These results might be due to small sample size of this study. Also, our data lack the exact history and duration of these comorbidities. Otherwise, these reports, together with those by Tiemeier et al. (2002, 2003) and Thomas et al. (2001), indicate the importance of investigating not only the presence/absence of hypertension but also other indices such as arterial stiffness and atheroma when considering risk factors for late-onset mood disorders. Therefore more detailed investigation of risk factors for cerebrovascular lesions may be needed in further studies.

As for the percentage of patients with obesity, there was significant difference between LOM and EOM. Depression and obesity frequently co-exist, and obesity can follow depression that occurred earlier in life (Bornstein et al.,

2006). Medications, particularly those commonly used in psychiatry and neurology, are a significant iatrogenic source of overweight and obesity (Aronne and Segal, 2003). In these regards, the higher percentage of patients with obesity in the EOM group might be caused by psychiatric medication during a longer period since the onset of a mood disorder.

There was negative correlation between the number of ECTs and the DWMH ratings. This result might be explained by the possibility that, because patients with severe DWMH rating have a poor response to ECT (Simpson et al., 1998; Steffens et al., 2001) and are predisposed to delirium (Figiel et al., 1990), frequent ECTs were avoided in the treatment for these patients, and the number of ECTs turned out to be lower in this population.

In summary, these findings in this study suggest that, in mood disorder patients, the time since the onset of disorder does not affect the development of white matter lesions, but that white matter lesions are associated with late-onset mood disorders. As for brain regions, it was also speculated that the frontal areas and the left parieto-occipital areas are important for the development of the late-onset type.

Our present findings indicate that various pre-existing risk factors including aging and (here undetected) medical comorbidities may have caused cerebrovascular lesions in these regions, which then resulted in depressive phenotype of LOM, and that early-onset type may be more closely associated with non-vascular factors like genetic elements. Prospective studies are needed to investigate whether cerebrovascular lesions surely induce depressive phenotype in later life. Furthermore, as the symptom spectrum of late onset mood disorders may be accompanied by cognitive impairment not closely analyzed in this study, the effect of these lesions on cognitive function should be examined.

Conflict of Interest

All authors declare that they have no conflicts of interest.

Role of funding source

Funding for this study was provided by a Health and Labor Sciences Research Grant for Research on Psychiatric and Neurological Diseases and Mental Health from the Japanese Ministry of Health, Labor and Welfare (MM); the Japanese Ministry of Health, Labor and Welfare had no further role in study design; in the collection, analysis and interpretation of data; in the writing of the report; and in the decision to submit the paper for publication.

Acknowledgements

The authors thank all the staff members of the various departments of Gunma University Hospital for their collaboration and Dr. Toru Uehara for helpful comments on the manuscript.

References

Alexopoulos GS, Young RC, Meyers BS. Geriatric depression: age of onset and dementia. Biological Psychiatry 1993;34:141–5.

Alexopoulos GS, Meyers BS, Young RC, Kakuma T, Feder M, Einhorn A, et al. Recovery in geriatric depression. Archives of General Psychiatry 1996;53:305–12.

Alexopoulos GS, Meyers BS, Young RC, Campbell S, Silbersweig D, Charlson M. Vascular depression hypothesis. Archives of General Psychiatry 1997;54:915–22.

Altshuler LL, Curran JG, Hauser P, Mintz J, Denicoff K, Post R. T2 hyperintensities in bipolar disorder: magnetic resonance imaging comparison and literature meta-analysis. American Journal of Psychiatry 1995;152:1139–44.

Aronne LJ, Segal KR. Weight gain in the treatment of mood disorders. Journal of Clinical Psychiatry 2003;64(Suppl 8):22–9.

Baldwin RC. Late life depression and structural brain changes: a review of recent magnetic resonance imaging research. International Journal of Geriatric Psychiatry 1993;8:115–23.

Baldwin RC. Is vascular depression a distinct sub-type of depressive disorder? A review of causal evidence. International Journal of Geriatric Psychiatry 2005;20:1–11.

Baldwin RC, Tomenson B. Depression in later life: a comparison of symptoms and risk factors in early and late onset cases. British Journal of Psychiatry 1995;167:649–52.

Bornstein SR, Schuppenies A, Wong M-L, Licinio J. Approaching the shared biology of obesity and depression: the stress axis as the locus of gene–environment interactions. Molecular Psychiatry 2006;11:892–902.

Brody AL, Barsom MW, Bota RG, Saxena S. Prefrontal-subcortical and limbic circuit mediation of major depressive disorder. Seminars in Clinical Neuropsychiatry 2001;6:102–12.

Coffey CE, Wilkinson WE, Weiner RD, Parashos IA, Djang WT, Webb MC, et al. Quantitative cerebral anatomy in depression: a controlled magnetic resonance imaging study. Archives of General Psychiatry 1993;50:7–16.

de Groot JC, de Leeuw FE, Oudkerk M, Hofman A, Jolles J, Breteler MMB. Cerebral white matter lesions and depressive symptoms in elderly adults. Archives of General Psychiatry 2000;57:1071–6.

de Leeuw FE, de Groot JC, Achten E, Oudkerk M, Ramos LM, Heijboer R, et al. Prevalence of cerebral white matter lesions in elderly people: a population based magnetic resonance imaging study. The Rotterdam Scan Study. Journal of Neurology, Neurosurgery, and Psychiatry 2001;70:9–14.

de Leeuw FE, de Groot JC, Oudkerk M, Witteman JC, Hofman A, van Gijn J, et al. Hypertension and cerebral white matter lesions in a prospective cohort study. Brain: a Journal of Neurology 2002;125:765–72.

Drevets WC. Neuroimaging and neuropathological studies of depression: implications for the cognitive-emotional features of mood disorders. Current Opinion in Neurobiology 2001;11:240–9.

Fazekas F, Chawluk JB, Alavi A, Hurtig HI, Zimmerman RA. MR signal abnormalities at 1.5 T in Alzheimer's dementia and normal aging. American Journal of Roentgenology 1987;149:351–6.

Figiel GS, Coffey CE, Djang WT, Hoffman Jr G, Doraiswamy PM. Brain magnetic resonance imaging findings in ECT-induced delirium. Journal of Neuropsychiatry and Clinical Neurosciences 1990;2:53–8.

Folstein MF, Maiberger R, McHugh PR. Mood disorder as a specific complication of stroke. Journal of Neurology, Neurosurgery, and Psychiatry 1977;40:1018–20.

Fossati P, Ergis AM, Allilaire JF. Executive functioning in unipolar depression: a review. L'Encephale 2002;28:97–107.

Friedman MJ, Bennet PL. Depression and hypertension. Psychosomatic Medicine 1977;39:134–42.

Fujikawa T, Yamawaki S, Touhouda Y. Incidence of silent cerebral infarction in patients with major depression. Stroke 1993;24: 1631–4.

Greenwald BS, Kramer-Ginsberg E, Krishnan KRR, Ashtari M, Aupperle PM, Patel M. MRI signal hyperintensities in geriatric depression. American Journal of Psychiatry 1996;153:1212–5.

Hickie I, Scott E, Wilhelm K, Brodaty H. Subcortical hyperintensities on magnetic resonance imaging in patients with severe depression: a longitudinal evaluation. Biological Psychiatry 1997;42:367–74.

Hopkinson G. A genetic study of affective illness in patients over 50. British Journal of Psychiatry 1964;110:244–54.

Iidaka T, Nakajima T, Kawamoto K, Fukuda H, Suzuki Y, Maehara T, et al. Signal hyperintensities on brain magnetic resonance imaging in elderly depressed patients. European Neurology 1996;36:293–9.

Jones-Webb R, Jacobs Jr DR, Flack JM, Liu K. Relationships between depressive symptoms, anxiety, alcohol consumption, and blood pressure: results from the CARDIA study. Coronary artery risk development in young adults study. Alcoholism, Clinical and Experimental Research 1996;20:420–7.

Krishnan KR, Goli V, Ellinwood EH, France RD, Blazer DG, Nemeroff CB. Leukoencephalopathy in patients diagnosed as major depressive. Biological Psychiatry 1988;23:519–52.

Krishnan KR, Hays JC, Tupler LA, George LK, Blazer DG. Clinical and phenomenological comparisons of late-onset and early-onset depression. American Journal of Psychiatry 1995;152:785–8.

Krishnan KR, Hays JC, Blazer DG. MRI-defined vascular depression. American Journal of Psychiatry 1997;154:497–501.

Kumar A, Miller D, Ewbank D, Yousem D, Newberg A, Samuels S, et al. Quantitative anatomical measures and comorbid medical illness in late-life depression. American Journal of Geriatric Psychiatry 1997;5:15–25.

Kumar A, Jin Z, Bilker W, Udupa J, Gottlieb G. Late-onset minor and major depression: early evidence for common neuroanatomical substrates detected by using MRI. Proceedings of the National Academy of Sciences of the United States of America 1998;95:7654–8.

Kumar A, Thomas A, Lavretsky H, Yue K, Huda A, Curran J, et al. Frontal white matter biochemical abnormalities in late-life major depression detected with proton magnetic resonance spectroscopy. American Journal of Psychiatry 2002;159:630–6.

Leboyer M, Henry C, Paillere-Martinot M-L, Bellivier F. Age at onset in bipolar affective disorders: a review. Bipolar Disorder 2005;7:111–8.

Lenze E, Cross D, McKeel D, Neuman RJ, Sheline YI. White matter hyperintensities and gray matter lesions in physically healthy depressed subjects. American Journal of Psychiatry 1999;156:1602–7.

Longstreth WT, Diehr P, Manolio TA, Beauchamp NJ, Jungreis CA, Lefkowitz D. Cluster analysis and patterns of findings on cranial magnetic resonance imaging of the elderly. Archives of Neurology 2001;58:635–40.

Lyness JM, Conwell Y, Nelson JC. Suicide attempts in elderly psychiatric inpatients. Journal of American Geriatrics Society 1992;40:320–4.

Manolio TA, Kronmal RA, Burke GL, Poirier V, O'Leary DH, Gardin JM, et al. Magnetic resonance abnormalities and cardiovascular disease in older adults: the cardiovascular health study. Stroke 1994;25:318–27.

Post F. Dementia, depression and pseudodementia. In: Benson DF, Blumer D, editors. Psychiatric aspects of neurologic disease. New York: Grune & Stratton; 1975.

Rodin G, Voshart K. Depression in the medically ill: an overview. American Journal of Psychiatry 1986;143:696–705.

Salloway S, Malloy P, Kohn R, Gillard E, Duffy J, Rogg J, et al. MRI and neuropsychological differences in early- and late-life-onset geriatric depression. Neurology 1996;46:1567–74.

Schultz B. Auszalunger in der Verwandtschaft von nach Erkrankungsalter und Geschlechtgrupierten Manisch-Depressiven. Archiv fur Psychiatrie und Nervenkrankheiten 1951;186:560–76.

Simpson S, Baldwin RC, Jackson A, Burns AS. Is subcortical disease associated with a poor response to antidepressants? Neurological, neuropsychological, and neuroradiological findings in late-life depression. Psychological Medicine 1998;28:1015–26.

Soares JC, Mann JJ. The anatomy of mood disorders: review of structural neuroimaging studies. Biological Psychiatry 1997;41:86–106.

Steffens DC, Conway CR, Dombeck CB, Wagner HR, Tupler LA, Weiner RD. Severity of subcortical gray-matter hyperintensity predicts ECT response in geriatric depression. The Journal of ECT 2001;17:45–9.

Steffens DC, Krishnan KRR, Crump C, Burke GL. Cerebrovascular disease and evolution of depressive symptoms in the cardiovascular health study. Stroke 2002;33:1636–44.

Strober M. Relevance of early age-of-onset in genetic studies of bipolar affective disorder. Journal of the American Academy of Child and Adolescent Psychiatry 1992;31:606–10.

Taylor WD, MacFall JR, Steffens DC, Payne ME, Provenzale JM, Krishnan KRR. Localization of age-associated white matter hyperintensities in late-life depression. Progress in Neuro-psychopharmacology and Biological Psychiatry 2003;27:539–44.

Tekin S, Cummings JL. Frontal-subcortical neuronal circuits and clinical neuropsychiatry: an update. Journal of Psychosomatic Research 2002;53:647–54.

Thomas AJ, Ferrier IN, Kalaria RN, Perry RH, Brown A, O'Brien JT. A neuropathological study of vascular factors in late-life depression. Journal of Neurology, Neurosurgery, and Psychiatry 2001;70:83–7.

Thomas AJ, Kalaria RN, O'Brien JT. Depression and vascular disease: what is the relationship? Journal of Affective Disorders 2004;79:81–95.

Tiemeier H, Bakker SLM, Hofman A, Koudstaal PJ, Breteler MMB. Cerebral haemodynamics and depression in the elderly. Journal of Neurology, Neurosurgery, and Psychiatry 2002;73:34–9.

Tiemeier H, Breteler MMB, van Popele NM, Hofman A, Witterman JCM. Late-life depression is associated with arterial stiffness: a population-based study. Journal of American Geriatrics Society 2003;51:1105–10.

Tupler LA, Krishnan KRR, McDonald WM, Dombeck CB, D'Souza S, David C, et al. Anatomic location and laterality of MRI signal hyperintensities in late-life depression. Journal of Psychosomatic Research 2002;53:665–76.

Videbech P. PET measurements of brain glucose metabolism and blood flow in major depressive disorder: a critical review. Acta Psychiatrica Scandinavica 2000;101:11–20.

Ylikowski A, Erkinjuntti T, Raininko R, Sarna S, Sulkava R, Tilvis R. White matter hyperintensities on MRI in the neurologically nondiseased elderly. Stroke 1995;26:1171–7.

Neurochemistry

JOURNAL OF NEUROCHEMISTRY | 2008 | 106 | 805–814 doi: 10.1111/j.1471-4159.2008.05489.x

Large-scale analysis of glucocorticoid target genes in rat hypothalamus

Hirohito Sato,*,†,‡ Yukio Horikawa,†,‡,§ Katsumi Iizuka,‡ Noriko Sakurai,* Takeshi Tanaka,* Nobuyuki Shihara,‡ Akihiko Oshima,*,¶ Jun Takeda†,‡,§ and Masahiko Mikuni*

*Department of Psychiatry and Human Behavior, Gunma University Graduate School of Medicine, Gunma, Japan

†Department of Diabetes and Endocrinology, Gifu University Graduate School of Medicine, Gifu, Japan

‡Laboratory of Medical Genomics, Institute for Molecular and Cellular Regulation, Gunma, Japan

§Core Research for Evolutional Science and Technology, Japan Science and Technology Corporation, Kawaguchi, Japan

¶Department of Psychiatry, Kitasato University School of Medicine, Kanagawa, Japan

Abstract

Insufficient glucocorticoid (GC) signaling is frequently observed in major depressive disorder (MDD). Since emotional and behavioral symptoms are often accompanied by disturbances in hypothalamic systems, GC insufficiency in this region is regarded as important in the pathogenesis of MDD. In this study, 22 early GC-responsive genes comprising 15 up-regulated and 7 down-regulated genes in rat hypothalamus were identified as being regulated at least two-fold by dexamethasone using microarray with 22 599 unique transcripts. Among these 22 genes, five of which are novel GC-responsive genes, the expression patterns of *sgk*, *bcl6*, *pdk4*, and *plekhf1* were examined *in vitro* in detail, and GC-responsive regions were identified only within the promoter of *sgk*. This suggests that glucocorticoid response element-independent pathways also play a critical role in early GC-response in hypothalamus. Considering that a number of these GC-responsive genes are candidate neuronal regulators, this gene list should be useful in clarifying the relationship between GC insufficiency and the pathogenesis of MDD.

Keywords: corticotropin releasing hormone, glucocorticoid response element, major depressive disorder, microarray.

J. Neurochem. (2008) **106**, 805–814.

Major depressive disorder (MDD) is a common psychiatric disorder responsible for substantial disability worldwide. The pathogenesis is not yet clear, although hypotheses including hypothalamus-pituitary-adrenal axis hyperactivity, impairment of serotonergic neurotransmission, and suppression of neurogenesis in hippocampus have been proposed. (Raison and Miller 2003, van Praag 2004, Lee *et al.* 2002).

Glucocorticoids are involved in various systemic physiological responses. Single GC treatment increases blood glucose, catabolism, some immunological responses, and neuronal action (Nestler *et al.* 2001). A series of GC exposures induces inappropriate effects in the whole body. Skin atrophy, osteoporosis, peptic ulcer, diabetes, growth retardation, and hypertension are observed (Schäcke *et al.* 2002). In CNS, neuronal apoptosis in hippocampus has been shown to be a chronic effect of GC treatment (Lee *et al.* 2002). According to the classic genomic theory of action, GCs bind to the glucocorticoid receptors (GRs), which are intracellular transcription factors. They exert positive or negative effects on the expression of target genes by either directly binding to DNA sequences as glucocorticoid response elements (GREs) or by indirectly modulating expression via protein–protein interaction with other transcription factors (Newton 2000). The earliest genomic GC effect was seen within 7.5 min, but diverse time lags in each

Received November 14, 2007; revised manuscript received May 5, 2008; accepted May 7, 2008.

Address correspondence and reprint requests to Yukio Horikawa MD, PhD, Department of Diabetes and Endocrinology, Gifu University Graduate School of Medicine, 1-1 Yanagido, Gifu 501-1194, Japan. E-mail: yhorikaw@gifu-u.ac.jp

Abbreviations used: CRH, corticotropin releasing hormone; DEX, dexamethasone; DEX-P, dexamethasone 21-phosphate disodium; DIG, digoxygenin; GC, glucocorticoid; GR, glucocorticoid receptor; GRE, glucocorticoid response element; ISH, *in situ* hybridization; MDD, major depressive disorder; pol2, polymerase (RNA) II (DNA directed) polypeptide A; PVN, paraventricular nucleus; SRC, steroid receptor co-activator; TFBS, transcription factor binding site.

gene from minutes to days were found (Falkenstein *et al.* 2000; Dean and Sanders 1996). In addition to genomic steroid action, there has been increasing evidence of non-genomic effects characterized by rapid onset of action (within seconds to minutes) (Falkenstein *et al.* 2000). The non-genomic effects on cellular function involve conventional second messenger cascades, mRNA stability, and protein degradation. (Newton 2000).

Insufficient GC signaling is found consistently in MDD patients (Raison and Miller 2003). The dexamethasone suppression test and its newer version, the dexamethasone–corticotropin releasing hormone (CRH) stimulation test, receive the most attention as biological markers for MDD diagnosis (Greden *et al.* 1983; Kunugi *et al.* 2006). Both tests have been shown to powerfully predict clinical response, and in the case of the dexamethasone-CRH test, there is evidence that impaired GC responsiveness represents a genetically based risk factor for the development of depression (Modell *et al.* 1998). In the field of human association studies, it was proposed that *FKBP5* (a GR-regulating co-chaperone of hsp-90) variant-dependent alterations in hypothalamus-pituitary-adrenal-axis regulation might be related to the shorter response time to antidepressant drug treatment as well as to the increased recurrence of depressive episodes (Binder *et al.* 2004). In addition, results of *in vitro* studies have shown that peripheral immune cells from MDD patients exhibit decreased *GR alpha* mRNA and decreased sensitivity to well-known immunosuppressive effects of GCs (Matsubara *et al.* 2006, Raison and Miller 2003). On the other hand, emotional and behavioral alterations such as sleep dysfunction and abnormal eating behavior are frequently seen in MDD patients. Because hypothalamus is characterized by its ability to regulate emotions and behaviors via both hormonal and neuronal pathways, abnormal function of hypothalamus might well be associated with the pathogenesis of MDD. Indeed, CRH hypersecretion in hypothalamic paraventricular nucleus is observed in MDD (Nemeroff *et al.* 1984; Catalán *et al.* 1998). As CRH induces emotional and behavioral effects in animals that include alterations in activity, appetite, and sleep, it has been suggested that CRH hypersecretion may partially contribute to emotional and behavioral alterations in MDD (Owens and Nemeroff 1991).

Glucocorticoid inhibition of hypothalamic neuronal activity appears at a relatively early phase in animals. Several investigators have detected GC inhibitory action of stress-induced paraventricular nucleus (PVN) neuronal activity and CRH transcription at 2 h after GC treatment in animals (Imaki *et al.* 1995; Lauand *et al.* 2007). However, the molecular mechanism is controversial. It has been reported that GC rapidly (3–5 min) inhibits glutaminergic afferents in PVN neurons of hypothalamic slices, most likely via a non-genomic pathway (Di *et al.* 2003). However, the genomic pathway seems also to be active in CRH suppression, since GRs are abundantly co-expressed with CRH in PVN. Indeed, specific GR-deficient mice are used to represent CRH over-expression and over-secretion in PVN (Uht *et al.* 1988; Tronche *et al.* 1999). These phenomena show that insufficient GC signaling increases CRH secretion in hypothalamus, as seen in MDD patients. Thus, insufficient GC signaling in hypothalamus may be an important feature of MDD pathophysiology.

In this study, we have comprehensively identified the early GC-responsive genes in hypothalamus, and suggest a mechanism whereby insufficient GC signaling might result in depression. In addition, this gene list comprises candidate genes linking depressive symptoms or vulnerability to MDD.

Materials and methods

Animals and treatment

Adult male Sprague-Dawley Rats (250–350 g, Charles River Japan, Yokohama, Japan) were used in all experiments. The animals were housed one per cage in a room with controlled temperature and a fixed lighting schedule (lights on from 6:00 a.m. to 6:00 p.m). Food and water were given *ad lib.* All experimental protocols were approved by the animal committee of Gunma University, Gunma, Japan.

Dexamethasone 21-phosphate disodium (DEX-P; Sigma, St. Louis, MO, USA) was used as DEX in the present study. The rats received a single intraperitoneal injection of either DEX-P in saline at a dose of 0.02, 0.2, or 2 mg/kg, or vehicle (1 mL/kg) from 10:00 a.m. to 1:00 p.m, and were killed by decapitation 2, 6 or 24 h later. Brains were dissected on ice. Using Brain Matrix (Brain Tree, Kingston, MA, USA) and razors, two coronal cuts were placed at the apex of the optic chiasm and the rostral margin of the mammillary bodies (5 mm slice). These slices were stored in RNAlater (Qiagen, Valencia, CA, USA) at −20°C. For *in situ* hybridization (ISH), brains from a number of the animals were rapidly frozen and molded on Tissuetek OCT compound (Sakura, Tokyo, Japan) in 2-methyl butane surrounded with liquid nitrogen, and stored at −80°C.

Microarray analysis

For dissecting hypothalamus, the slice treated with RNAlater was placed flat, and cuts were placed on either side of the optic tracts. Final cut was placed just above the third ventricle. Total RNA from hypothalamus of the animals 2 h after injection (six rats treated with 2 mg/kg DEX-P and six rats treated with vehicle) was extracted using an RNeasy Plus Mini Kit (Qiagen). These 12 RNA samples were divided into four pools including two DEX-treated pools and two control pools. Each pool was constructed with samples from three animals. Rat Genome 230 2.0 Array (Affymetrix, Santa Clara, CA, USA) was used. This rat expression array comprises 31 000 probe sets designed to detect 22 599 unique transcripts. Four arrays were prepared for four pools. Double-stranded cDNA derived from 1.6 μg of total RNA was used to produce biotinylated cRNA, and labeled cRNA targets were hybridized to GeneChips. Hybridization was allowed to proceed 16 h at 45°C, followed by washing and staining with streptavidin–phycoerythrin. Hybridization assay procedures including preparation of solutions were carried out as described in the Affymetrix GeneChip Expression Analysis Technical Manual. The distribution of fluorescent material on the array was obtained using GeneArray Scanner 3000 (Affymetrix).

Microarray Suite (MAS) version 5.0 and GeneChip Operating Software (GCOS) supplied by Affymetrix was used to perform gene expression analysis. Details of analyses are shown in *Data analysis*.

Computed prediction of glucocorticoid response elements

A computational tool, rVISTA 2.0, was used to predict putative GREs of the GC-responsive genes screened by microarray (http://rvista.dcode.org/). This program was developed for high-throughput discovery of *cis*-regulatory elements, and combines clustering of predicted transcription factor binding sites (TFBSs) and the analysis of interspecies sequence conservation to maximize the identification of functional sites (Loots and Ovcharenko 2004). It uses available position weight matrices in the TRANSFAC database v10.2 and MATCH program that can detect potential sequence matches by automatic searches with precompiled matrices (http://www.biobase.de). DNA sequences from 10 kb upstream of the putative transcription initiation sites of the candidate genes were extracted. The 5′-end of the Refseq sequences were used as the putative transcription initiation sites. For luciferase assay, transcription of these 5′-UTR regions of *sgk*, *bcl6*, *pdk4*, and *plekhf1* was confirmed by RT-PCR using adequate primers. These sequences were subsequently entered into ecrbrowser of rVISTA 2.0. Matrices of GREs (GR_Q6, GRE_C, GR) were used and analyzed in the evolutionally conserved sequences between rat and human genomes. The optimized value was used for a cut-off parameter corresponding to not more than 3 TFBSs per 10 kb of a random sequence.

Semi-quantitative RT-PCR

Total RNA from each animal was extracted by the same method as described in Microarray analysis, and reverse-transcripted using first strand cDNA synthesis kit (Invitrogen, Carlsbad, CA, USA). TaqMan primers and probes were designed by Applied Biosystems (Foster City, CA, USA), Serum/glucocorticoid regulated kinase (*sgk*) : Rn00570285_m1, Pyruvate dehydrogenase kinase 4 (*pdk4*) : Rn00585577_m1, Pleckstrin homology domain containing family F (with FYVE domain) member 1 (*plekhf1*) : Rn01475628_s1, b-cell leukemia/lymphoma 6 (*bcl6*) FAM: 5′- CCGTACCATTGTGAGAAG-3′, *bcl6* forward (F): 5′-CGCATCCACACAGGAGAGAA-3′, *bcl6* reverse (R) : 5′-CTTTTGTGACGAAAGTGCAGGTT-3′, polymerase (RNA) II (DNA directed) polypeptide A (*pol2*) FAM: 5′-ACACACCGAGTTCAC-3′, *pol2* F: 5′-CCCTCGAGCCCACGGTATA-3′, *pol2* R: 5′-ACTCTGGTGAGCTAGGACTGTAGGA-3′. TaqMan reactions were performed in a reaction volume of 20 μL using components supplied in a TaqMan PCR reagent kit. Each reaction consisted of 10 μL TaqMan Universal Master Mix, 900 nM of each amplification primer, and 250 nM of the corresponding TaqMan probe. Each sample was run for an initial 2 min at 50 °C and 10 min at 95 °C, followed by 40 cycles at 95 °C for 15 s and at 60 °C for 1 min. Amplification data were collected by the 7700 Sequence Detector and analyzed using Sequence Detection System software (Applied Biosystems).

Luciferase assay

Plasmid construction

The rat *sgk* promoter (KpnI- -1,207/+115 -KpnI), *bcl6* promoter (KpnI- -3211/+52 -BglII), *pdk4* promoter (*Hin*dIII- -2,982/+75 -*Hin*dIII), and *plekhf1* promoter (*Hin*dIII- -1,179 /+100 -*Hin*dIII) were generated by PCR with rat genome using restriction site linked primers shown in Supplementary material Table S1, and inserted into the pGEM-Teasy (Promega, Madison, WI, USA). These plasmids were treated with appropriate restriction enzymes and constructed by cloning into pGL3-basic (Promega). Triple putative GRE sequences of *sgk* and *plekhf1* (sgk GRE: GCGGAAAGGACAGAATGTTCTCGGAGA, plekhf1 GRE: CACAGCAGTGCATTTTGTAAATGTTTA) also were cloned into pGL3-promoter vector (Promega). All constructs were confirmed by sequencing.

Cell culture and transient expression assays

Hela cells were incubated 2 days in 12-well plates with Dulbecco's modified Eagle's medium without serum. These cells were transfected with 1.8 μg of each promoter construct, 0.2 μg pRL-TK, and 6.6 μL ExGen 500 *in vitro* transfection reagent (Fermentas, Hanover, MD, USA). Cells were subsequently incubated for 24 h with or without 1 μM DEX. 24 h after transfection, cells were lysed in 250 μL of 1 × Passive reporter lysis buffer (Promega). Luciferase activities were measured using a Dual-luciferase reporter assay system (Promega). All transfection studies were performed in four independent experiments and repeated twice.

In situ hybridization (ISH)

The cDNA fragments of the rat genes were obtained by PCR using the primers shown in Supplementary material Table S2, and subcloned into the pGEM T-easy vector (Promega). The digoxygenin (DIG)-labeled riboprobes were produced using these plasmids as templates for *in vitro* transcription. Riboprobes were purified by ProbeQuant 50 spin column (Amersham Biosciences, Little Chalfont, UK) and ethanol precipitation.

Brains molded on Tissuetek OCT compound were cryosectioned at 12 μm thickness. Briefly, after postfixation, acetylation, and prehybridization, sections were hybridized with a DIG-RNA probe (0.5 μg/mL) in a hybridization buffer (50% formamide, 5 × SSC, 5 × Denhardt's solution, 250 μg/mL yeast RNA, and 500 μg/mL salmon sperm DNA) at 72°C for 18 h. Following posthybridization wash in 0.2 × SSC at 72°C, the sections were incubated with an anti-DIG antibody conjugated with alkaline phosphatase (1/1,000, Roche Diagnostics, Tokyo, Japan). The sections were washed in TNT (0.1 M Tris–HCl, pH 7.5, 0.15 M NaCl, 0.1% Tween 20) three times for 5 min and once in TS 9.5 (0.1 M Tris–HCl, pH 9.5, 0.1 M NaCl, 50 mM $MgCl_2$), and the alkaline phosphatase activity was detected using a NBT/BCIP system (Roche Diagnostics) according to the manufacturer's instructions. The incubation for this substrate was carried out for 16 h and stopped by washing twice for 5 min in phosphate-buffered saline containing 0.5 mM EDTA. After dehydration, the sections were prepared with Entellan neu (Merck, Darmstadt, Germany). The images for the ISH were obtained by digital color camera DP-50 (Olympus, Tokyo, Japan) attached to a BX-51 microscope (Olympus).

Data analysis

In the present study, two microarray experiments were performed using two DEX-treated pools and two control pools. Prior to performing data comparison, the data were normalized against total intensity to correct for variations in overall intensity and heteroge-

neity among the GeneChip probe arrays. Two sets of algorithms were generated and used to generate change significance and change quantity metrics for each probe set using MAS version 5.0. The change algorithm generated a Change p-value and an associated fold-change value. The second algorithm gave a quantitative estimate of the change in gene expression in the form of Signal Log Ratio. In the present study, the level of gene expression was regarded as increased when its Change p-value was less than 0.0025 (two-fold); gene expression was regarded as decreased when its Change p-value was greater than 0.9975 (two-fold). Fold change was calculated by the following formula: Fold change $= 2^{(\text{signal log ratio})}$.

Other statistical analyses were performed using the SPSS program. Student's t-test was used to compare Taqman PCR data (delta CT) at each time point between DEX-treated animals and controls, and luciferase activity between DEX-treated cells and controls (p-value < 0.05). One-way ANOVA and Dunnet's multiple comparison analysis was used to compare Taqman PCR data (delta CT) between animals treated with each DEX dose (p-value < 0.05).

Results

Screening of GC-responsive genes

Duplicate experiments reproductively identified 22 known genes, five hypothetical proteins, and nine ESTs as genes regulated at least two-fold by DEX using the Affymetrix microarray. Only the known genes are shown in Table 1. 17 (77%) of these 22 genes (*gadd45g*, *sgk*, *pdk4*, *nfkbia*, *errfi1*, *dusp1*, *bcl6*, *ddit4*, *gpd1*, *thbs1*, *mt1a*, *cxcr4*, *sox9*, *tnfrsf11b*, *id3*, *cga*, and *hes5*) already have been reported to be GC-responsive in extra-hypothalamic tissues or some cell lines (Agbemafle *et al.* 2005; Maiyar *et al.* 1997; Huang *et al.* 2002; Deroo and Archer 2001, Xu *et al.* 2005; Kassel *et al.* 2001; Stojadinovic *et al.* 2007, Wang *et al.* 2003; Cheng and de Vellis 2000, Leclerc *et al.* 2004; Kelly *et al.* 1997; Nagase *et al.* 2000, Sekiya *et al.* 2001; Kondo *et al.* 2007; Hurson *et al.* 2007; Akerblom *et al.* 1988; Lee *et al.* 2007), while the others are newly identified as GC- responsive (*Plekhf1*,

Table 1 Glucocorticoid-responsive genes in rat hypothalamus following acute dexamethasone treatment

Probe ID	Gene title	Symbol	FC1	FC2	Ave	GRE	References
1388792_at	Growth arrest and DNA-damage-inducible 45 gamma	Gadd45g	5.3	5.3	5.3		Agbemafle *et al.* (2005)
1367802_at	Serum/glucocorticoid regulated kinase	Sgk	4.6	4.9	4.8	GRE	Maiyar *et al.* (1997)
1369150_at	Pyruvate dehydrogenase kinase, isoenzyme 4	Pdk4	4.3	2.6	3.5	GRE	Huang *et al.* (2002)
1389538_at	Nuclear factor of kappa light chain gene enhancer in B-cells inhibitor, alpha	Nfkbia	3.5	3.0	3.3		Deroo and Archer (2001)
1373532_at	Pleckstrin homology domain containing, family F (with FYVE domain) member 1	Plekhf1	3.2	2.6	2.9		
1373093_at	ERBB receptor feedback inhibitor 1	Errfi1	3.0	2.6	2.8		Xu *et al.* (2005)
1383608_at	Arrestin domain containing	Arrdc2	3.5	2.0	2.7		
1368146_at	Dual specificity phosphatase 1	Dusp1	2.6	2.6	2.6	GRE	Kassel *et al.* (2001)
1374446_at	TCDD-inducible poly(ADP-ribose) polymerase (predicted)	Tiparp_ predicted	2.6	2.6	2.6		
1379368_at	B-cell leukemia/lymphoma 6 (predicted)	Bcl6_ predicted	2.6	2.3	2.5	GRE	Stojadinovic et al. (2007)
1368025_at	DNA-damage-inducible transcript 4	Ddit4	2.5	2.5	2.5		Wang *et al.* (2003)
1369560_at	Glycerol-3-phosphate dehydrogenase 1 (soluble)	Gpd1	2.5	2.1	2.3	GRE	Cheng and de Vellis (2000)
1374529_at	Thrombospondin 1	Thbs1	2.3	2.0	2.1		Leclerc *et al.* (2004)
1382732_at	Extracellular link domain-containing 1 (predicted)	Xlkd1_ predicted	2.3	2.0	2.1		
1371237_a_at	Metallothionein 1a	Mt1a	2.1	2.1	2.1	GRE	Kelly *et al.* (1997)
1370973_at	Sodium channel, voltage-gated, type VII, alpha	Scn7a	−2.0	−2.0	−2.0		
1373661_a_at	Chemokine (C-X-C motif) receptor 4	Cxcr4	−2.5	−2.0	−2.2		Nagase *et al.* (2000)
1392813_at	SRY-box containing gene 9	Sox9	−2.3	−2.6	−2.5		Stojadinovic *et al.* (2007)
1387769_a_at	Inhibitor of DNA binding 3	Id3	−2.8	−2.5	−2.6	GRE	Hurson *et al.* (2007)
1369407_at	Tumor necrosis factor receptor superfamily, member 11b (osteoprotegerin)	Tnfrsf11b	−4.0	−2.1	−3.1		Kondo *et al.* (2007)
1369659_at	Glycoprotein hormones, alpha subunit	Cga	−2.8	−4.0	−3.4	GRE	Akerblom *et al.* (1988)
1368942_at	Hairy and enhancer of split 5 (*Drosophila*)	Hes5	−4.0	−3.7	−3.9		Lee *et al.* (2007)

Genes regulated by DEX. Only known genes altered at least two-fold are listed. Filled column for GRE indicates a previous report or rVISTA prediction of a GRE within the gene. The column of reference indicates that investigators have shown the GC-response of these genes previously. Abbreviations in this table are FC1: fold-change of experiment 1, FC2: fold-change of experiment 2, Ave: average value of fold-change in both experiments.

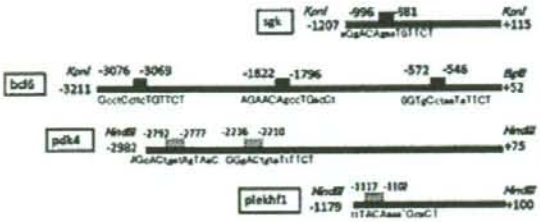

Fig. 1 GR binding sites were predicted by rVISTA ver. 2.0. Black and grey rectangles represent putative GREs conserved between rat and human and putative GREs conserved between rat and mouse, respectively. The base positions and sequences of GREs are attached. Sequences common to consensus GRE are capitalized. Adequate restriction enzymes are linked to the primers for subcloning of these regions. These sequences were inserted into pGL3-basic vector.

Arrdc2, Tiparp, Xlkd1, Scn7a). Among the 22 known genes, 15 were up-regulated and 7 were down-regulated.

In silico prediction of GREs with the GC-up-regulated genes screened by microarray

rVISTA 2.0 predicted GREs in the promoter regions of 2 of the 15 up-regulated genes. *Sgk* and *bcl6* were predicted to have one and three putative GREs within 10 kb upstream of the transcription start site, respectively. The sites of predicted GREs and their consensus sequences are shown in Fig. 1.

Semi-quantitative RT-PCR

The change of expression levels of *sgk, bcl6, pdk4,* and *plekhf1* as determined by the microarray by 2 mg/kg DEX treatment were confirmed by Taqman RT-PCR. The expression level of *sgk, bcl6, pdk4,* and *plekhf1* were increased 5.2-fold ($p < 0.001$), 4.0-fold ($p < 0.001$), 18-fold ($p < 0.001$), and 2.8-fold ($p < 0.001$) respectively. The expression level of *sgk* and *bcl6* were also significantly induced by 0.2 mg/kg DEX 3.4-fold ($p < 0.05$) and 1.8-fold ($p < 0.05$), respectively. However, no significant regulation was detected with *pdk4* and *plekhf1* mRNA by 0.2 mg/kg DEX treatment. No change of expression levels of these genes was detected by 0.02 mg/kg DEX treatment ($n = 4$) (Fig. 2a–d). As shown in Fig. 2e–h, the expression levels of all four genes were altered most strongly within 2 h after injection of DEX, and returned to baseline 24 h after injection. The fold changes of *sgk* expression 6 and 24 h after 2 mg DEX treatment (compared with vehicle) were 2.5 ± 0.2 (1.0 ± 0.3, $p < 0.001$) and 1.1 ± 0.2 (1.0 ± 0.1), while those of *bcl6* were 2.7 ± 0.2 (1.0 ± 0.1, $p < 0.001$) and 1.0 ± 0.1 (1.0 ± 0.3), those of *pdk4* were 7.7 ± 2.0 (1.0 ± 0.4, $p < 0.001$) and 1.0 ± 0.3 (1.0 ± 0.5), and those of *plekhf1* were 2.5 ± 0.3 (1.0 ± 0.1, $p < 0.001$) and 0.9 ± 0.1 (1.0 ± 0.1) (average value of control rats in each time was defined as 1, average ± SD, $n = 4$).

The effect of GCs on *sgk, bcl6, pdk4,* and *plekhf1* promoter activity

Luciferase activity of *sgk* was increased 2.56-fold ($n = 8$, $p < 0.05$) by 1 μM DEX in Hela cells (Fig. 3a). However, luciferase assay failed to detect an increase in promoter activity of *bcl6, pdk4, and plekhf1*. Luciferase activity of the promoter vector with the triple putative GRE of *sgk* also was

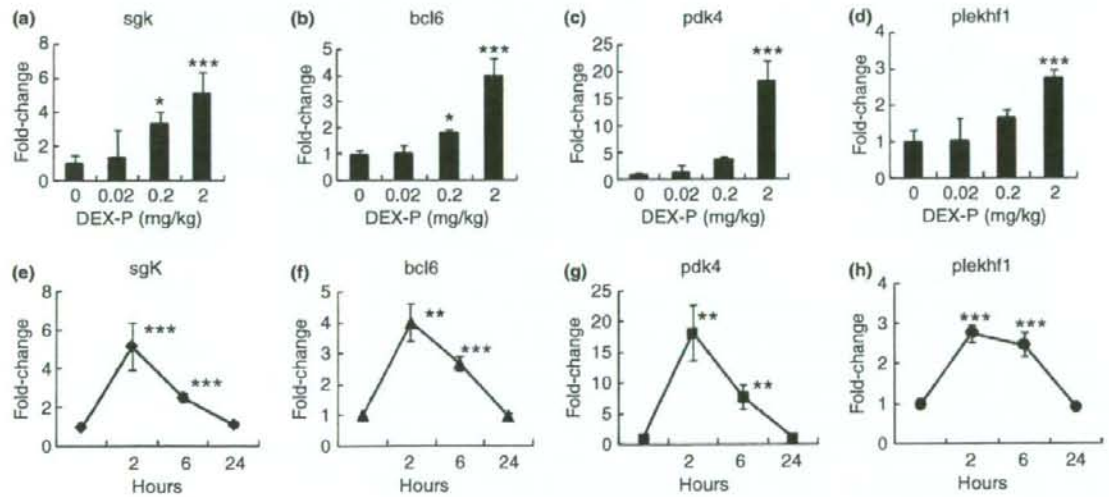

Fig. 2 Taqman RT-PCR confirmed microarray data on four GC-responsive genes. Change values of these genes were dependent on DEX dose. Average quantity of vehicle-treated animals was defined as 1 (a–d). Maximum alteration was detected at 2 h after treatment with all of these genes. Average quantity of vehicle-treated animals at each time point was defined as 1 (e–h). Statistics are described in Data analysis ($n = 4$, $^*p < 0.05$, $^{**}p < 0.01$, $^{***}p < 0.001$, the bars indicate SD).

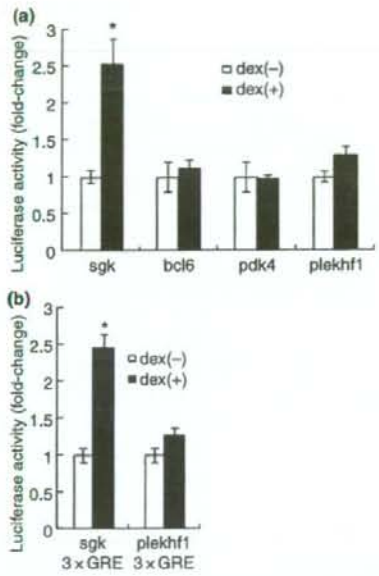

Fig. 3 Luciferase activity of each promoter in Fig. 1 is shown in (a) ($n = 8$). Luciferase activity of 3 × GRE of *sgk* and *plekhf1* with promoter vector is shown in (b) ($n = 12$). Promoter activity of these promoters incubated with (solid colums) or without (open colums) 1 μM DEX were compared. Average quantity of luciferase activity without DEX was defined as 1 ($p < 0.05$, the bars indicate SD).

increased 2.46-fold ($n = 12, p < 0.05$) by 1 μM DEX in Hela cells, but no response was observed with that of *plekhf1* (Fig. 3b).

Localization of GC-responsive genes in hypothalamus

The expression of *sgk* was detected by ISH in all of the hypothalamic areas diffusely, but substructures could not be distinguished. *Bcl6* was detected in all of the hypothalamic cells also stained by Toluidine blue, i.e., in all neuronal cells in hypothalamus. While *pdk4* and *plekhf1*, like *sgk*, were detected diffusely, they were most strongly detected in PVN. All of the four selected genes were detected in PVN (Fig. 4).

Discussion

This study is the first comprehensive report elucidating the genes rapidly regulated by GC in rat hypothalamus. Using microarray, we have identified targets of GC signaling in hypothalamus. This list contains new candidate genes associated with depressive symptoms and vulnerability to MDD. Microarray was used in this study since our preliminary study showed it was capable of comprehensive detection of approximately 90% of known genes expressed in hypothalamus in comparison with cDNA library sequencing (data not shown). Microarray detected 22 GC-responsive genes in rat hypothalamus. Thresholds of fold-change varied from 1.4 to 2.5 in previous reports using microarray to

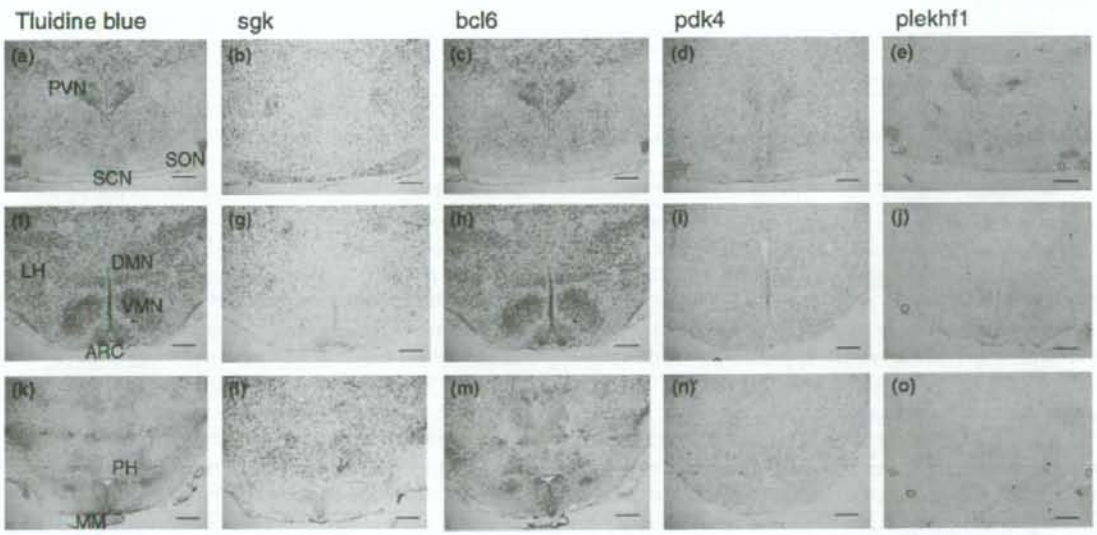

Fig. 4 Representative *in situ* hybridization images of the glucocorticoid responsive genes are shown. Brains of DEX-treated animals were cryosectioned ($n = 2$), and slices of anterior (a–e), medial (f–j), and posterior (k–o) regions of hypothalamus were prepared. Tluidine blue stain was used as guides to hypothalamic nuclei (a, f, k). Antisense riboprobes for *sgk* (b, g, l), *bcl6* (c, h, m), *pdk4* (d, i, n), *plekhf1* (e, j, o) were hybridized as indicated in Materials and methods. Scale bars indicate 500 μm. Abbreviations used in this figure are SCN: suprachiasmatic nucleus, SON: supra optic nucleus, DMN: dorsomedial nucleus, VMN: ventromedial nucleus, ARC: arcuate nucleus, LH: lateral hypothalamus, PH: posterior hypothalamus, MM: mammilary body.

identify GC-responsive genes (Agbemafle *et al.* 2005; Leclerc *et al.* 2004). In the present study, the threshold was fixed at two-fold since the rate of reproduction in duplication was 0.71, 0.71, 0.65 and 0.60, respectively, by fixing the threshold at four-fold, two-fold, 1.74-fold, and 1.51-fold, respectively. 15 genes were up-regulated and 7 genes were down-regulated. These included five transcription factors or cofactors, four signal transducers, and two enzymes of glucose metabolism. However, only three reports have been published that identify early GC-responsive genes within 2 h after DEX treatment (Wu *et al.* 2004; Agbemafle *et al.* 2005; Stojadinovic *et al.* 2007). Of these, two give lists of genes regulated at least two-fold. Agbemafle *et al.* (2005) detected 102 GC-responsive genes in intestine regulated at least 1.4-fold at 2 h after intraperitoneal DEX injection in neonatal mice. Among these, only 20 genes were regulated at least two-fold. The main functions were signal transduction, transcription, cell proliferation, cell death, development, and metabolism. Stojadinovic *et al.* (2007) detected 23 GC-responsive genes in human keratinocytes at 1 h after DEX treatment. The main functions were almost the same as in the previous report. The number and main function of the genes regulated in this study were similar to those of two previous reports, although the number of commonly identified genes was small, three between neonatal intestine and hypothalamus and three between keratinocytes and hypothalamus. 17 of the 22 genes (77%) already have been described as GC-responsive in some published article, suggesting that this experiment was properly done. Although a larger number of DEX responsive genes has been reported at later time points (Wang *et al.* 2004; Stojadinovic *et al.* 2007), we chose the earlier time point because evidence of GC response in hypothalamus was limited to early responses such as DEX suppression of hypothalamic activity. In our pilot study, DEX suppression was detected 2 h after DEX treatment, as in two previous reports (data not shown) (Imaki *et al.* 1995; Lauand et al. 2007). In addition, in our pilot study, 2 mg/kg of DEX significantly suppressed the plasma concentration of corticosterone 2 h after DEX treatment, while 0.2, 0.02 mg/kg of DEX did not (data not shown). 2 mg/kg was therefore selected as an effective dosage and was used for the microarray experiments. Indeed, TaqMan RT-PCR data show that a 0.2 mg/kg (1/10 dose) of DEX failed to regulate three of four selected genes more than two-fold.

Because the GC-response via the classic DNA-dependent genomic pathway requires a GRE within the 5′- flanking region, we examined the validity of screening for primary GR targets by predicting GREs *in silico*. Since several studies have shown that non-coding regulatory sequences tend to be evolutionarily conserved, we used rVISTA, a TFBS searching program with multispecies comparative sequence alignments, for predicting putative GREs (Hardison 2000; Wasserman *et al.* 2000). GR binding sites have been found in both up-regulated and down-regulated genes. However, the negative GREs in down-regulated genes are less similar to the consensus sequence, and the mechanism of transrepression such as interaction with other transcription factor activity is more complex. Accordingly, we concentrated on up-regulated genes. Among 15 up-regulated genes, the program predicted GREs in 2 genes (13%), *sgk* and *bcl6*, within evolutionarily conserved regions. Because of the rigid algorithm of rVISTA, oversight of GREs was considered, as Meng *et al.* (2006) reported. Searching published descriptions of the remaining 13 up-regulated genes of any species, we extracted an additional four genes, *pdk4*, *dusp1*, *gpd1*, and *mt1a*, holding GREs. (Kwon *et al.* 2004; Kassel *et al.* 2001; Cheng and de Vellis 2000; Kelly *et al.* 1997). Thus, six genes (40%) are candidate GR primary targets and nine genes (60%) are regulated by GC not having a GRE region. These six genes, all candidate GR primary targets, consist of three signal transducers, one transcription factor, and two enzymes of glucose metabolism. We selected three of these candidate genes for GR target, *sgk*, *bcl6*, and *pdk4*, which are GC-regulated most strongly in each category, respectively, to be examined for details of expression patterns. Taqman RT-PCR confirmed dose-dependency and early response of these genes to GC. However, luciferase assay confirmed GRE activity only of the *sgk* gene, as previously shown by Maiyar *et al.* (1997). The promoter region of *sgk* overlapped with that confirmed by Maiyer *et al.*, and the promoter of *bcl6* was homologous to that cloned by Ohashi *et al.* (1995) in human. In addition, the 5′-UTR region of *pdk4* was partially homologous to the human *pdk4* used by Kwon *et al.* (2004). The suitable regions were selected to construct plasmids as promoters. Although Kwon *et al.* (2004) confirmed a GRE region (-864/-809) of human *pdk4* promoter by gel shift assay and luciferase assay, the luciferase assay in this study failed to confirm GRE activity of rat *pdk4* promoter. This may be due to the remarkable differences between the promoter regions of human and rat *pdk4* promoter as described by Kwon and Harris (2004). They also predicted a putative GRE located 6 kb upstream of rat *pdk4* promoter using MatInspector program (another TFBS predicting program) and gel shift assay, suggesting that the shorter *pdk4* promoter of this study was one of the reasons for this non-responsiveness. Although GREs of these two genes are not active in Hela cells, the possibility cannot be excluded that they are active in other cell lines. Ma *et al.* (2006) detected binding between putative ChoRE and ChREBP (a transcription factor regulating metabolic enzymes) within the 5′- flanking region of the *gpdh* gene by gel shift assay. Their luciferase assay failed to confirm activity of the putative ChoRE, but Ma *et al.* pointed out the possibility that the ChoRE activity of *gpdh* requires other active components to construct a complex. GR also constructs complexes with co-activators including steroid receptor co-activators (SRCs) SRC-1a, SRC-1e, SRC-2, and SRC-3. In addition, expression of co-activators is

tissue-specific, and recruitment of SRCs is promoter-sensitive and also -specific (Grenier *et al.* 2004). Thus, Hela cells lack crucial co-activators for a GC-response of *bcl6* and *pdk4*. Wang *et al.* (2004) screened 71 GC-responsive genes in A549 cells by microarray. A following GR RNA interference experiment failed to suppress the GC-response of about 29 of these genes (41%), indicating a lack of GR action. Rapid neurophysiological and behavioral effects of GCs have been identified that share signaling pathways with second messengers including Ca^{2+} and Protein kinase C and some of these are not affected by classic antagonists of GR (RU-38486) (Falkenstein *et al.* 2000). Such non-genomic pathways are also implicated by GC action of *pdk4* and *bcl6*. Another possibility for this non-responsiveness is that these two genes are secondary responsive genes downstream of other primary GC targets. Although secondary responsive genes should be regulated at a more delayed time point (Dean and Sanders 1996), at least one secondary responsive gene, *hes5*, was detected among 22 GC responsive genes. Lee *et al.* (2007) have found *hes5* up-regulation by inactive mutant sgk transfection in rat hippocampus. In this study, *hes5* repression was simultaneously detected together with *sgk* induction. This accords with that reported in hippocampus, in which part of the secondary response has begun within 2 h. Further experiments using cycloheximide, an inhibitor of protein synthesis, are required to discriminate primary and secondary effects.

A number of these GC-responsive genes have been reported to be associated with early GC effects in extrahypothalamic tissues. For example, Tsai *et al.* (2002) have shown that sgk facilitates memory consolidation in hippocampus, and acute stress affects this phenomenon. In addition, sgk suppresses insulin secretion within 4 h of DEX treatment in pancreatic beta cells (Ullrich *et al.* 2005). On the other hand, *tnfrsf11b*, an osteoporosis sensitive gene (Arko *et al.* 2002), is regulated by single DEX treatment. Since osteoporosis is known to be caused by long-term GC treatment and not by single treatment (Schäcke *et al.* 2002), some of these GC-responsive genes may be associated with GC effects only through a series of treatments.

Five GC-responsive genes were newly identified in this study, *plekhf1*, *arrdc2*, *tiparp*, *xlkd1*, and *scn7a*. Among these, we selected *plekhf1*, the most increased gene of these five, to be examined in detail with *sgk*, *bcl6*, and *pdk4*. We confirmed the GC response of this gene by TaqMan RT-PCR and the expression in the hypothalamus by ISH. Although rVISTA failed to identify GREs in the conserved genomic region between rat and human within 10 kb upstream of the *plekhf1* promoter, this program calculated a putative GRE in the conserved region between rat and mouse at 1.1 kb upstream. The results of the luciferase assay using 1.2 kb of the promoter region suggests no GC impact on promoter activity. Assay using the promoter vector with triple putative GRE sequences also indicates that this GRE is inactive. Although it is possible that additional GREs are present at locations more distant than 10 kb or in introns, the GC response of *plekhf1* most likely occurs via GRE-independent pathways. *Plekhf1* was first identified by Chen *et al.* (2005) as a lysosome-associated apoptosis-inducing protein containing the plekstrin homology and FYVE domains (LAPF). They found expression of *plekhf1* in human and mouse brain by northern blot and RT-PCR, respectively (Chen *et al.* 2005). The detection of *plekhf1* expression in hypothalamus in this study accords with their analysis. Although the known function of *plekhf1* is restricted to induction of apoptosis in fibrosarcoma cells (Chen *et al.* 2005), this gene also has been reported as a gene induced by eyeblink conditioning in cerebellum together with *sgk* (Park *et al.* 2006). In addition, an elevated GC level was found to occur in the acquisition of conditioning (Shors *et al.* 1992). Together with the *plekhf1* response to GCs in this study, the gene is a novel candidate gene linking GC and acquisition of conditioning, and may also be a novel GC responsive neuronal regulator.

This gene list contains both suppressors of peptide secretion and inhibitors of cytokine transcription, so a number of these genes may be related to neuronal activity in hypothalamus. Since *sgk*, *bcl6*, *pdk4*, and *plekhf1* were also detected in PVN by ISH, these genes would seem to be involved in GC action of CRH suppression. Sgk has been shown to regulate a variety of ion channels including potassium channels such as voltage-gated Kv channels in kidney and pancreatic beta cells (Lang *et al.* 2003; Ullrich *et al.* 2005). DEX suppresses insulin release in insulin secreting cells via Kv 1.5 channel activity up-regulation (Ullrich *et al.* 2005). In addition, *Kv 1.5* mRNA was abundantly detected by the microarray in hypothalamus. Because an increase of Kv channel activity represses neuronal excitability (Malin and Nerbonne 2001), and CRH secretion requires neuronal activity of PVN, an increase of potassium channel activity via sgk might well reduce CRH secretion. However, the mechanism of CRH secretion remains unclear. There are numerous points in the multiple molecular processes at which GC might inhibit CRH secretion, such as neuronal afferent sets, CRH transcription and peptide synthesis, membrane excitability, etc. (Watts 2005). While these candidates are not yet proved to regulate CRH secretion, this study has identified genes 'responding to GC in hypothalamus', which is a crucial requirement of feedback regulators of CRH secretion.

In summary, we have comprehensively identified early GC-responsive genes in hypothalamus using microarray. GC-responsive promoter activity was confirmed with only one of these genes, *sgk*, by luciferase assay. This indicates that GRE-independent pathways including non-genomic pathways and secondary effects also play a critical role in the early GC-response in hypothalamus. In addition, the novel GC target gene *plekhf1* was identified, which is possibly links GC and change in neuronal activity. Considering that a

number of these genes are candidate neuronal regulators, this gene list is a useful resource for clarifying the relationship between GC insufficiency and the pathogenesis of MDD.

Acknowledgments

This work was supported by a Health and Labor Science Research Grant for research on Psychiatric and Neurological Diseases and Mental Health from the Japanese Ministry of Health, Labor and Welfare. This study was also supported by Grant-in-Aid for Scientific Research from the Japanese Ministry of Science, Education, Sports, Culture and Technology and in part by the New Energy and Industrial Technology Development Organization. We thank Hiroshi Kunugi for help in microarray experiments, and Motoko Uchiyama for technical support in animal experiments.

Supplementary material

The following supplementary material is available for this article:

Table S1 PCR primers (plasmid construction for luciferase assay).

Table S2 PCR primers (ISH probe synthesis).

This material is available as part of the online article from: http://www.blackwell-synergy.com/doi/abs/10.1111/j.1471-4159.2008.05489.x (This link will take you to the article abstract).

Please note: Blackwell Publishing is not responsible for the content or functionality of any supplementary materials supplied by the authors. Any queries (other than missing material) should be directed to the corresponding author for the article.

References

Agbemafle B. M., Oesterreicher T. J., Shaw C. A. and Henning S. J. (2005) Immediate early genes of glucocorticoid action on the developing intestine. *Am. J. Physiol. Gastrointest. Liver Physiol.* **288**, G897–G906.

Akerblom I. E., Slater E. P., Beato M., Baxter J. D. and Mellon P. L. (1988) Negative regulation by glucocorticoids through interference with a cAMP responsive enhancer. *Science* **241**, 350–353.

Arko B., Prezelj J., Komel R., Kocijancic A., Hudler P. and Marc J. (2002) Sequence variations in the osteoprotegerin gene promoter in patients with postmenopausal osteoporosis. *J. Clin. Endocr. Metab.* **87**, 4080–4084.

Binder E. B., Salyakina D., Lichtner P. *et al.* (2004) Polymorphisms in FKBP5 are associated with increased recurrence of depressive episodes and rapid response to antidepressant treatment. *Nat. Genet.* **36**, 1319–1325.

Catalán R., Gallart J. M., Castellanos J. M. and Galard R. (1998) Plasma corticotropin-releasing factor in depressive disorders. *Biol. Psychiatry* **44**, 15–20.

Chen W., Li N., Chen T., Han Y., Li C., Wang Y., He W., Zhang L., Wan T. and Cao X. (2005) The lysosome-associated apoptosis-inducing protein containing the pleckstrin homology (PH) and FYVE domains (LAPF), representative of a novel family of PH and FYVE domain-containing proteins, induces caspase-independent apoptosis via the lysosomal-mitochondrial pathway. *J. Biol. Chem.* **280**, 40985–40995.

Cheng J. D. and de Vellis J. (2000) Oligodendrocytes as glucocorticoids target cells: functional analysis of the glycerol phosphate dehydrogenase gene. *J. Neurosci. Res.* **59**, 436–445.

Dean D. M. and Sanders M. M. (1996) Ten years after: reclassification of steroid-responsive genes. *Mol. Endocrinol.* **10**, 1489–1495.

Deroo B. J. and Archer T. K. (2001) Glucocorticoid receptor activation of the I kappa B alpha promoter within chromatin. *Mol. Biol. Cell* **12**, 3365–3374.

Di S., Malcher-Lopes R., Halmos K. C. and Tasker J. G. (2003) Nongenomic glucocorticoid inhibition via endocannabinoid release in the hypothalamus: a fast feedback mechanism. *J. Neurosci.* **23**, 4850–4857.

Falkenstein E., Tillmann H. C., Christ M., Feuring M. and Wehling M. (2000) Multiple actions of steroid hormones–a focus on rapid, nongenomic effects. *Pharmacol. Rev.* **52**, 513–556.

Greden J. F., Gardner R., King D., Grunhaus L., Carroll B. J. and Kronfol Z. (1983) Dexamethasone suppression tests in antidepressant treatment of melancholia. The process of normalization and test-retest reproducibility. *Arch. Gen. Psychiatry* **40**, 493–500.

Grenier J., Trousson A., Chauchereau A., Amazit L., Lamirand A., Leclerc P., Guiochon-Mantel A., Schumacher M. and Massaad C. (2004) Selective Recruitment of p160 Coactivators on Glucocorticoid-Regulated Promoters in Schwann Cells. *Mol. Endocrinol.* **18**, 2866–2879.

Hardison R. C. (2000) Conserved noncoding sequences are reliable guides to regulatory elements. *Trends Genet.* **16**, 369–372.

Huang B., Wu P., Bowker-Kinley M. M. and Harris R. A. (2002) Regulation of pyruvate dehydrogenase kinase expression by peroxisome proliferator-activated receptor-alpha ligands, glucocorticoids, and insulin. *Diabetes* **51**, 276–283.

Hurson C. J., Butler J. S., Keating D. T., Murray D. W., Sadlier D. M., O'Byrne J. M. and Doran P. P. (2007) Gene expression analysis in human osteoblasts exposed to dexamethasone identifies altered developmental pathways as putative drivers of osteoporosis. *BMC Musculoskelet. Disord.* **8**, 12.

Imaki T., Xiao-Quan W., Shibasaki T., Yamada K., Harada S., Chikada N., Naruse M. and Demura H. (1995) Stress-induced activation of neuronal activity and corticotropin-releasing factor gene expression in the paraventricular nucleus is modulated by glucocorticoids in rats. *J. Clin. Invest.* **96**, 231–238.

Kassel O., Sancono A., Krätzschmar J., Kreft B., Stassen M. and Cato A. C. (2001) Glucocorticoids inhibit MAP kinase via increased expression and decreased degradation of MKP-1. *EMBO J.* **20**, 7108–7116.

Kelly E. J., Sandgren E. P., Brinster R. L. and Palmiter R. D. (1997) A pair of adjacent glucocorticoid response elements regulate expression of two mouse metallothionein genes. *Proc. Natl Acad. Sci. USA* **94**, 10045–10050.

Kondo T., Kitazawa R., Yamaguchi A. and Kitazawa S. (2007) Dexamethasone promotes osteoclastogenesis by inhibiting osteoprotegerin through multiple levels. *J. Cell. Biochem.* **103**, 335–345.

Kunugi H., Ida I., Owashi T. *et al.* (2006) Assessment of the dexamethasone/CRH test as a state-dependent marker for hypothalamic-pituitary-adrenal (HPA) axis abnormalities in major depressive episode: a Multicenter Study. *Neuropsychopharmacology* **31**, 212–220.

Kwon H. S. and Harris R. A. (2004) Mechanisms responsible for regulation of pyruvate dehydrogenase kinase 4 gene expression. *Adv. Enzyme Regul.* **44**, 109–121.

Kwon H. S., Huang B., Unterman T. G. and Harris R. A. (2004) Protein kinase B-alpha inhibits human pyruvate dehydrogenase kinase-4 gene induction by dexamethasone through inactivation of FOXO transcription factors. *Diabetes* **53**, 899–910.

Lang F., Henke G., Embark H. M., Waldegger S., Palmada M., Bohmer C. and Vallon V. (2003) Regulation of channels by the serum and glucocorticoid-inducible kinase – implications for transport, excitability and cell proliferation. *Cell Physiol. Biochem.* **13**, 41–50.

Lauand F., Ruginsk S. G., Rodrigues H. L. P., Reis W. L., de Castro M., Elias L. L. K. and Antunes-Rodrigues J. (2007) Glucocorticoid modulation of atrial natriuretic peptide, oxytocin, vasopressin and Fos expression in response to osmotic, angiotensinergic and cholinergic stimulation. *Neuroscience* **147**, 247–257.

Leclerc N., Luppen C. A., Ho V. V., Nagpal S., Hacia J. G., Smith E. and Frenkel B. (2004) Gene expression profiling of glucocorticoid-inhibited osteoblasts. *J. Mol. Endocrinol.* **33**, 175–193.

Lee A. L., Ogle W. O. and Sapolsky R. M. (2002) Stress and depression: possible links to neuron death in the hippocampus. *Bipolar Disord.* **4**, 117–128.

Lee C. T., Ma Y. L. and Lee E. H. (2007) Serum- and glucocorticoid-inducible kinase1 enhances contextual fear memory formation through down-regulation of the expression of Hes5. *J. Neurochem.* **100**, 1531–1542.

Loots G. G. and Ovcharenko I. (2004) rVISTA 2.0: evolutionary analysis of transcription factor binding sites. *Nucleic Acids Res.* **32** (Web Server Issue), W217–W221.

Ma L., Robinson L. N. and Towle H. C. (2006) ChREBP•Mlx Is the Principal Mediator of Glucose-induced Gene Expression in the Liver. *J. Biol. Chem.* **281**, 28721–28730.

Maiyar A. C., Phu P. T., Huang A. J. and Firestone G. L. (1997) Repression of Glucocorticoid Receptor Transactivation and DNA Binding of a Glucocorticoid Response Element within the Serum/Glucocorticoid-Inducible Protein Kinase (sgk) Gene Promoter by the p53 Tumor Suppressor Protein. *Mol. Endocrinol.* **11**, 312–329.

Malin S. A. and Nerbonne J. M. (2001) Molecular heterogeneity of the voltage-gated fast transient outward K+ current, I(Af), in mammalian neurons. *J. Neurosci.* **21**, 8004–8014.

Matsubara T., Funato H., Kobayashi A., Nobumoto M. and Watanabe Y. (2006) Reduced Glucocorticoid Receptor alpha Expression in Mood Disorder Patients and First-Degree Relatives. *Biol. Psychiatry* **59**, 689–695.

Meng H., Banerjee A. and Zhou L. (2006) BLISS: biding site level identification of shared signal-modules in DNA regulatory sequences. *BMC Bioinformatics* **7**, 287.

Modell S., Lauer C. J., Schreiber W., Huber J., Krieg J. C. and Holsboer F. (1998) Hormonal response pattern in the combined DEX-CRH test is stable over time in subjects at high familial risk for affective disorders. *Neuropsychopharmacology* **18**, 253–262.

Nagase H., Miyamasu M., Yamaguchi M., Kawasaki H., Ohta K., Yamamoto K., Morita Y. and Hirai K. (2000) Glucocorticoids preferentially upregulate functional CXCR4 expression in eosinophils. *J. Allergy Clin. Immunol.* **106**, 1132–1139.

Nemeroff C. B., Widerlov E., Bissette G., Walleus H., Karlsson I., Eklund K., Kilts C. D., Loosen P. T. and Vale W. (1984) Elevated concentrations of CSF corticotropin-releasing factor-like immunoreactivity in depressed patients. *Science* **226**, 1342–1344.

Nestler E. J., Hyman S. E. and Malenka R. C. (2001) *Molecular Neuropharmacology : A Foundation for Clinical Neuroscience*. McGraw-Hill Companies, Inc., New York.

Newton R. (2000) Molecular mechanisms of glucocorticoid action: what is important? *Thorax* **55**, 603–613.

Ohashi K., Miki T., Hirosawa S. and Aoki N. (1995) Characterization of the promoter region of human BCL-6 gene. *Biochem. Biophys. Res. Commun.* **214**, 461–467.

Owens M. J. and Nemeroff C. B. (1991) Physiology and pharmacology of corticotropin-releasing factor. *Pharmacol. Rev.* **43**, 425–473.

Park J. S., Onodera T., Nishimura S., Thompson R. F. and Itohara S. (2006) Molecular evidence for two-stage learning and partial laterality in eyeblink conditioning of mice. *Proc. Natl Acad. Sci. USA* **103**, 5549–5554.

van Praag H. M. (2004) Can stress cause depression? *Prog. Neuropsychopharmacol. Biol. Psychiatry* **28**, 891–907.

Raison C. L. and Miller A.H. (2003) When not enough is too much: the role of insufficient glucocorticoid signaling in the pathophysiology of stress-related disorders. *Am. J. Psychiatry* **160**, 1554–1565.

Schäcke H., Döcke W. D. and Asadullah K. (2002) Mechanisms involved in the side effects of glucocorticoids. *Pharmacol. Ther.* **96**, 23–43.

Sekiya I., Koopman P., Tsuji K., Mertin S., Harley V., Yamada Y., Shinomiya K., Nifuji A. and Noda M. (2001) Dexamethasone enhances SOX9 expression in chondrocytes. *J. Endocrinol.* **169**, 573–579.

Shors T. J., Weiss C. and Thompson R.F. (1992) Stress-induced facilitation of classical conditioning. *Science* **257**, 537–539.

Stojadinovic O., Lee B., Vouthounis C., Vukelic S., Pastar I., Blumenberg M., Brem H. and Tomic-Canic M. (2007) Novel genomic effects of glucocorticoids in epidermal keratinocytes: inhibition of apoptosis, interferon-gamma pathway, and wound healing along with promotion of terminal differentiation. *J. Biol. Chem.* **282**, 4021–4034.

Tronche F., Kellendonk C., Kretz O., Gass P., Anlag K., Orban P. C., Bock R., Klein R. and Schütz G. (1999) Disruption of the glucocorticoid receptor gene in the nervous system results in reduced anxiety. *Nat. Genet.* **23**, 99–103.

Tsai K. J., Chen S. K., Ma Y. L., Hsu W. L. and Lee E. H. (2002) sgk, a primary glucocorticoid-induced gene, facilitates memory consolidation of spatial learning in rats. *Proc. Natl Acad. Sci. USA* **99**, 3990–3995.

Uht R. M., McKelvy J. F., Harrison R. W. and Bohn M.C. (1988) Demonstration of glucocorticoid receptor-like immunoreactivity in glucocorticoid-sensitive vasopressin and corticotropin-releasing factor neurons in the hypothalamic paraventricular nucleus. *J. Neurosci. Res.* **19**, 405–411.

Ullrich S., Berchtold S., Ranta F. *et al.* (2005) Serum- and glucocorticoid-inducible kinase 1 (SGK1) mediates glucocorticoid-induced inhibition of insulin secretion. *Diabetes* **54**, 1090–1099.

Wang Z., Malone M. H., Thomenius M. J., Zhong F., Xu F. and Distelhorst C. W. (2003) Dexamethasone-induced gene 2 (dig2) is a novel pro-survival stress gene induced rapidly by diverse apoptotic signals. *J. Biol. Chem.* **278**, 27053–27058.

Wang J. C., Derynck M. K., Nonaka D. F., Khodabakhsh D. B., Haqq C. and Yamamoto K. R. (2004) Chromatin immunoprecipitation (ChIP) scanning identifies primary glucocorticoid receptor target genes. *Proc. Natl Acad. Sci. USA* **101**, 15603–15608.

Wasserman W. W., Palumbo M., Thompson W., Fickett J. W. and Lawrence C. E. (2000) Human-mouse genome comparisons to locate regulatory sites. *Nat. Genet.* **26**, 225–228.

Watts A. G. (2005) Glucocorticoid regulation of peptide genes in neuroendocrine CRH neurons: a complexity beyond negative feedback. *Front. Neuroendocrinol.* **26**, 109–130.

Wu W., Chaudhuri S., Brickley D. R., Pang D., Karrison T. and Conzen S. D. (2004) Microarray analysis reveals glucocorticoid-regulated survival genes that are associated with inhibition of apoptosis in breast epithelial cells. *Cancer Res.* **64**, 1757–1764.

Xu D., Makkinje A. and Kyriakis J. M. (2005) Gene 33 is an endogenous inhibitor of epidermal growth factor (EGF) receptor signaling and mediates dexamethasone-induced suppression of EGF function. *J. Biol. Chem.* **280**, 2924–2933.

Psychophysiology, *46* (2009), 52–61. Wiley Periodicals, Inc. Printed in the USA.

DOI: 10.1111/j.1469-8986.2008.00748.x

Preattentive dysfunction in major depression: A magnetoencephalography study using auditory mismatch negativity

YUICHI TAKEI,[a] SUMIE KUMANO,[a] SUGURU HATTORI,[a] TORU UEHARA,[a] YUKI KAWAKUBO,[b] KIYOTO KASAI,[b] MASATO FUKUDA,[a] AND MASAHIKO MIKUNI[a]

[a]Department of Psychiatry and Human Behavior, Gunma University Graduate School of Medicine, Gunma, Japan
[b]Department of Neuropsychiatry, Tokyo University Graduate School of Medicine, Tokyo, Japan

Abstract

Information processing deficits in major depressive disorder have been infrequently examined electrophysiologically. Its preattentive and sensory information processing was examined using mismatch field (MMNm) and P1m components, respectively, by magnetoencephalography. Fourteen major depressive disorder patients and 19 healthy volunteers participated in the study. MMNm was elicited in response to duration and frequency changes of pure-tone stimuli and in response to a vowel across-category change. The magnetic global field power (mGFP) of MMNm was significantly smaller in the major depressive disorder patients than in the healthy volunteers, although that of P1m did not differ between the two groups. Information processing at the preattentive level is impaired functionally in major depressive disorder, and this dysfunction is not due to the dysfunction at the lower level of information processing.

Descriptors: MEG, Mismatch negativity, Major depressive disorder, MMN, Magnetoencephalography, Attention

Cognitive dysfunctions are assumed to underlie clinical symptoms in major depressive disorder patients and have been included in the criteria for establishing diagnosis: For example, a diminished ability to think or concentrate during a major depressive episode is included as an item in the *Diagnostic and Statistical Manual of Mental Disorders*, fourth edition (*DSM-IV*). Cognitive dysfunctions in major depressive disorder patients have been experimentally demonstrated in many neuropsychological studies. During a depressive episode of major depressive disorder patients, neuropsychological deficits have been demonstrated in memory, learning, attention, alertness, and executive functions (Austin et al., 1992; Veiel, 1997; Zakzanis, Leach, & Kaplan, 1998). In addition, a number of recent studies have shown that some of these cognitive deficits persist during the euthymic state and symptomatological remission (Austin et al., 1992; Tham et al., 1997).

Information processing deficits underlying these cognitive dysfunctions in major depressive disorder patients can be examined electrophysiologically using event-related potentials (ERPs). For example, among late ERPs, the P300 component has often been reported to be reduced in amplitude and delayed in peak latency in major depressive disorder patients (Karaaslan, Gonul, Oguz, Erdinc, & Esel, 2003; Kawasaki, Tanaka, Wang, Hokama, & Hiramatsu, 2004; Papageorgiou et al., 2004; Roschke & Wagner, 2003; Urretavizcaya et al., 2003), and the results are interpreted as reflecting abnormalities in the capacity of attentional operation resource (Kok, 2001). However, because late ERPs such as P300 are often vulnerable to motivational factors and task involvement of the participants, the interpretation of these findings in major depressive disorder patients is difficult.

Among the earlier components of ERPs, mismatch negativity (MMN) has been the most extensively investigated to elucidate preattentive cognitive function. MMN and its magnetic counterpart (MMNm) are considered to reflect preattentive information processing and are elicited approximately 150–200 ms after the onset of physically deviant auditory stimuli in identical and repeated stimulus sequences (Hari et al., 1984; Näätänen, Gaillard, & Mäntysalo, 1978). Although there is some evidence for attentional modulation of MMN (Trejo, Ryan-Jones, & Kramer, 1995; Woldorff, Hillyard, Gallen, Hampson, & Bloom, 1998), MMN is elicited even when attention is directed away from the auditory input. Thus, the significance of MMN results can be more easily interpreted than that of P300 results if the motivational factor of the subjects cannot be controlled, as in the case of psychiatric patients. This automatic mismatch process might have an important role in initiating an involuntary switching of attention to an auditory stimulus change occurring outside the focus of attention (Giard, Perrin, Pernier, & Bouchet, 1990; Lyytinen, Blomberg, & Näätänen, 1992; Näätänen, 1992).

Among various psychiatric disorders, MMN has been studied mainly in schizophrenia. In a meta-analysis of MMN (Umbricht & Krljes, 2005), it was concluded that MMN deficits are a robust

We thank Dr. Masato Yumoto of the Tokyo University Graduate School of Medicine for his collaboration in this study.

Address reprint requests to: Masato Fukuda, 3-39-22 Showa, Maebashi, Gunma 371-8511, Japan. E-mail address: fkdpsy@med.gunma-u.ac.jp

feature of chronic schizophrenia and represent the underlying mechanism of attention dysfunction in schizophrenia. Studies of MMNm in schizophrenia also indicated an MMNm amplitude decrease in schizophrenia and changes in the equivalent current dipole (ECD) location (Kasai et al., 2003; Kreitschmann-Andermahr et al., 1999; Oades et al., 2006; Pekkonen et al., 2002).

There have been few studies of MMN in major depressive disorder patients. Umbricht et al. (2003) examined MMN generated in response to a pure-tone duration and a frequency change in major depressive disorder patients, bipolar disorder patients, schizophrenia patients, and in healthy volunteers and found no significant differences in MMN amplitude between major depressive disorder patients and healthy volunteers. Ogura, Nageishi, and Omura (1995) investigated major depressive disorder patients and bipolar disorder patients in the depressive state using the oddball paradigm of a tone-burst frequency change. They reported that the mean amplitude of the early N200 component (N2a), which corresponds to the MMN component, of the patients in the depressive state was smaller than that of the healthy volunteers. Lepistö et al. (2004) investigated MMN using a consonant sound change and a novel sound and found a short MMN latency and an unchanged MMN amplitude in children with major depressive disorder patients compared with those in healthy children. Taken together, these previous studies of MMN in major depressive disorder patients have not yielded sufficiently consistent results.

Another earlier ERP component, P1, often called P50, and its magnetic counterpart P1m are considered to reflect earlier stages of auditory information processing and, in accordance with the assumption, its dipole is located in the primary auditory cortex. This component is employed in studies of auditory information processing in psychiatric disorders. For example, Ahveninen et al. (2006) reported a significant P50 amplitude reduction and a marked deviation of P50m dipole sources in a twin study of schizophrenia, and assumed that a P50 amplitude reduction and a P50m dipole deviation might be a marker of brain function changes related to the genetic predisposition to schizophrenia and that these changes might be inherited as morphological changes in auditory cortex neurons. In fact, from these findings, the left superior temporal gyrus and left medial temporal lobe are considered to be key regions of structural difference in patients with schizophrenia (Honea, Crow, Passingham, & Mackay, 2005).

Whole-head magnetoencephalography (MEG) has advantages over scalp electroencephalography (EEG) in terms of its higher spatial resolution with many recording channels and its more accurate estimation of MMNm dipole locations. These advantages are due to the fact that magnetic fields are less affected by intervening tissues of different conductivities than electrical fields. To the best of our knowledge, there has been only one study of MMNm and P1m in major depressive disorder patients using MEG (Kähkönen et al., 2007). They used a pure-tone frequency deviant to elicit MMNm and found no significant differences in MMN amplitude or latency between major depressive disorder patients and healthy volunteers. In this study, we recorded MMNm and P1m by MEG in major depressive disorder patients in the passive oddball paradigms of vowel sounds as well as pure tone and examined their power and latency in relation to clinical symptoms and psychotropic medications. We also estimated the current dipoles of MMNm and P1m. Our hypotheses are as follows: (1) Preattentive information processing deficits are revealed as reduced MMNm power and/or delayed MMNm latency in major depressive disorder patients and (2) the locations of estimated current dipoles do not differ between major depressive disorder patients and healthy volunteers because most voxel-based morphometry studies showed no anatomical differences in temporal structures between major depressive disorder patients and healthy volunteers (Beyer & Krishnan, 2002).

Methods

Participants

Fourteen major depressive disorder patients and 19 healthy volunteers participated in this study (Table 1). The major depressive disorder patients were recruited from the Department of Psychiatry, Gunma University Hospital, Japan. Each patient was diagnosed as having major depressive disorder in accordance with *DSM-IV* (American Psychiatric Association, 1994).

The major depressive disorder patients included 9 men and 5 women (age: mean, 41.4 years; *SD*, 10.2; range, 25–60). Major depressive disorder patients over 60 years old were not included in this study to eliminate the effects of additional pathophysiological factors on major depressive disorder such as aging and vascular changes.

During this study, all the subjects were euthymic or depressive, as indicated by their 17-item Hamilton Rating Scale for Depression (HRSD) scores (mean, 10.7; *SD*, 4.1; range, 5–19; Hamilton, 1960). According to the minimental state examination (MMSE) scores, there were no patients with dementia in the major depressive disorder group. However, 13 of the 14 patients were on medication with antidepressants, mood stabilizers, antipsychotics, anxiolytics, or hypnotics during this study. The imipramine equivalent dose of antidepressants, the diazepam equivalent dose of anxiolytics, and the flunitrazepam equivalent dose of hypnotics were calculated for each patient (Inagaki & Inada, 2006).

The healthy volunteers included 13 men and 6 women (age: mean, 37.7 years; *SD*, 10.0; range, 26–56). They had no history of any major psychiatric disorders or major physical illnesses and were not on any major psychiatric medications during this study. The mean age and sex ratio did not significantly differ between the two groups, $F(1,31) = 1.0$, $p = .32$; $\chi^2(1) = 0.62$, $p = .80$. All the subjects were right-handed as indicated by their Edinburgh inventory scores (mean, 96.8; *SD*, 6.0; range, 80–100; Oldfield, 1971). Their sleepiness scores at the time of MEG examination were assessed using the Stanford sleepiness scale. The sleepiness scores before, $F(1,31) = 0.29$, $p = .59$, and during the task performance, $F(1,31) = 1.52$, $p = .23$, did not differ significantly between the two groups.

For both the patients and healthy volunteers, Japanese was the first language. The exclusion criteria for both groups included clear abnormality of MRI results, neurological illness, traumatic brain injury with any of the known cognitive consequences or loss of consciousness for more than 5 min, substance use or addiction, and presence of hearing or vision impairment. This study was approved by the Institutional Review Board of Gunma University Hospital, and written informed consent was obtained from all the participants prior to the study.

Task Procedures

P1m and MMNm were recorded during an auditory task while the subjects were instructed to perform another visual task and to ignore the auditory stimuli.

Table 1. *Characteristics of Participants*

Case	Age (years)	Sex	Age of onset (years)	MMSE score	HRSD score	Total imipramine equivalent dose (mg/day)	Antidepressant (imipramine equivalent dose)	Mood stabilizer (mg/day)	Others (mg/day)
Major depressive disorder (n = 14)									
1	41	M	39	29	10	25	Sulpiride 50(25)		Zopiclone 7.5, Loflazepate 1
2	37	M	34	30	10	72.9	Milnacipran 100(66.7), Trazodone 25(12.5)		Nitrazepam 5
3	31	F	28	29	8	0			Loflazepate 1
4	37	M	24	29	6	75	Amitriptyline 75(75)	Lithium 600	Lorazepam 1, Zolpidem 5
5	37	M	36	30	13	60	Maprotiline 60(60)	Lithium 600	Lorazepam 1
6	54	F	24	30	9	112.5	Milnacipran 75(50), Sulpiride 100(50), Trazodone 25(12.5)		Clonazepam 1, Etizolam 1.5
7	58	M	57	29	7	25	Sulpiride 50(25)		Loflazepate 1
8	34	M	33	30	9	37.5	Paroxetine 10(37.5)		Levothyroxine 25
9	48	F	45	29	19	150	Paroxetine 40(150)		Quetiapine 100, Clonazepam 1.5, Nitrazepam 20, Quazepam 15, Flunitrazepam 2, Levothyroxine 25
10	42	F	20	30	12	125	Milnacipran 75(50), Amoxapine 75(75)		Etizolam 1.5
11	25	F	24	28	13	82.5	Milnacipran 30(20), Trazodone 125(62.5)	Valproate 200	Levomepromazine 5
12	40	M	34	30	11	300	Imipramine 150(150), Setiptiline 6(150)		Methylphenidate 10, Brotizolam 0.25, Triazolam 0.5, Flunitrazepam 2
13	60	M	34	30	18	141.7	Sulpiride 150(75), Maprotiline 25(25), Trazodone 25(12.5), Paroxetine 20(75)		
14	35	M					Sulpiride 150(75), Milnacipran 100(66.7)		Etizolam 1.5
Mean	41.4	M9/F5	34.6	29.5	10.7	99.6			
SD	10.2		10.9	0.7	4.1	79			
Healthy control (n = 19)									
Mean	37.7	M13/F6							
SD	10.0								

Note: M: male; F: female; HRSD: 17-item Hamilton Rating Scale for Depression.

Auditory mismatch negativity task. In the auditory task, the subjects were presented with sequences of auditory stimuli consisting of standard and deviant stimuli delivered randomly. The interstimulus interval was 445 ± 15 ms. The stimuli were delivered binaurally through plastic tubes. The experiment consisted of two conditions. The first condition was designed to elicit MMNm in response to duration and frequency changes of pure-tone stimuli (standard: 50-ms duration, 1000-Hz frequency, probability = 83%; duration deviant: 100-ms duration, 1000-Hz frequency, probability = 8.5%; frequency deviant: 50-ms duration, 1200-Hz frequency, probability = 8.5%). The second condition was designed to elicit MMNm in response to a vowel across-category change condition (standard, Japanese vowel sound/a/, probability = 90%; deviant, Japanese vowel sound/o/, probability = 10%). These vowel stimuli were spoken by a native Japanese, digitized using the NeuroStim system (NeuroScan, USA), and edited to have a loudness of 80 dBSPL and a rise/fall time of 10 ms. The frequency spectra for the vowels were as follows./a/: formant (F) 0 = 140, F1 = 760, F2 = 1250, F3 = 2750, and F4 = 3600 Hz;/o/: F0 = 140, F1 = 480, F2 = 770, F3 = 2820, and F4 = 3600 Hz. The frequency of the pure-tone stimuli was 1000 Hz, nearly equal to the central frequency of the formants of the vowel stimuli. The order of the two conditions was counterbalanced across the subjects.

Visual task. The subjects performed a visual task while ignoring the auditory stimuli during MMNm measurement. The visual stimuli consisted of three sequences. Sequence 1 consisted of pictures of animals, flowers, buildings, and fruits. Sequence 2 consisted of pictures of sweets, flowers, animals, insects, castles, festivals, stone lanterns, and fruits. Sequence 3 consisted of pictures of birds, landscapes, flowers, and roads. The target pictures of Sequence 1 were animals, those of Sequence 2 were sweets, and those of Sequence 3 were birds. In each sequence, the target pictures were randomly presented with a probability of 30%. The pictures were sequentially presented at 2000-ms duration on a screen placed 1.7 m from the subjects. The subjects were instructed to press a button immediately after a target

picture was presented. The order of the three sequences was counterbalanced across the subjects.

Data Acquisition

MEG. Magnetic fields were recorded in a magnetically shielded room (JFE Mechanical Co., Japan) with a 306-channel magnetometer (Knuutila et al., 1993). This whole-head magnetometer consisted of 102 triple-sensor units, each with two orthogonal planar gradiometers and one magnetometer that records maximal signals directly above the source (Hämäläinen, Hari, Ilmoniemi, Knuutila, & Lounasmaa, 1993). We used a 204-channel gradiometer for data analysis except for a 102-channel magnetometer, because we could not record the data obtained with the 102-channel magnetometer for all subjects. A subject was instructed to sit on a chair with his/her head inside the helmet-shaped magnetometer. The position of the magnetometer with respect to the head was determined at the beginning of the task under each condition according to the magnetic fields produced by currents fed into three indicator coils at predetermined locations on the scalp. The locations of these coils in relation to the preauricular points and nasion were determined with an Isotrak 3D digitizer (Polhemus TM, USA) before the start of the experiment.

MEG epochs were averaged separately for standard and deviant stimuli. The duration of the averaging period was 420 ms, including a 100-ms prestimulus baseline. The recording bandpass range was 0.1–100 Hz, with a sampling rate of 512 Hz. The first 10 stimuli were automatically excluded from averaging. MEG epochs exceeding 3000 fT/cm were also excluded from averaging. Data collection under each condition lasted until 100 deviant stimuli that did not generate artifacts were presented. This number for averaging was adopted according to those adopted in previous studies (Alho et al., 1998; Kasai et al., 2003) and considering the balance between the signal-to-noise ratio and a possible habituation effect of MMN in response to speech sound (McGee et al., 2001). Average responses were digitally filtered in the bandpass range of 1–20 Hz.

Magnetic resonance imaging (MRI) of brain. In all the major depressive disorder patients and volunteers, a set of 2-mm-thick, sagittal MRI slices were acquired with 1.5-T equipment (MAGNETOM Symphony Maestro Class, Siemens Medical Solutions, Erlangen, Germany) using a three-dimensional (3D) fast spoiled gradient recalled acquisition in the steady state (FSPGR). The MEG coordinate system was aligned with the MRI-based coordinates by identifying the left and right preauricular points, as well as the nasion, from the MRI slices.

Data Analysis

Magnetic counterpart of global field powers (mGFPs) of P1m and MMNm. The mismatch reaction is defined as the difference between the magnetic field of the standard tone and the evoked field of the deviant tone. The magnetic fields of standard tones were subtracted from those of deviant tones for each channel, and the root mean squares of the differences over the 54 channels positioned over the temporal region (Figure 1) were calculated for each subject as the magnetic counterpart of the global field power (mGFP) of the mismatch reaction, separately for each condition and hemisphere, using the formula shown in Figure 2 (Kreitschmann-Andermahr et al., 1999; Lehmann & Skrandies, 1980). The peak latency of P1m was determined as the maximum amplitude of the individual mGFP curve of standard stimuli for each condition between 40 and 100 ms (Tervaniemi et al., 1999). The individual curves of MMNm were calculated by subtracting the wave at each channel elicited in response to the standard tone from that elicited in response to deviant tones under the same experimental condition (Alho et al., 1998). The peak latency of MMNm was determined as the maximum amplitude of the individual mGFP curves between 100 and 250 ms (Kasai et al., 2003; Tervaniemi et al., 1999). The individual curve whose peak amplitude could not be found in the designated periods of those of P1m and MMNm was excluded from analysis.

$$\mathrm{mGFP\ (fT/cm)} = \sqrt{\frac{1}{n} \cdot \sum_{i=1}^{n} \left(Ui - \frac{\sum_{j=1}^{n} Uj}{n} \right)^2}$$

Figure 1. Grand mean waveform of magnetic fields for MMNm response to duration changes of pure-tone stimuli in major depressive disorder patients and healthy volunteers. Thick circles indicate selected channels. Thin circle indicates an enlarged picture of part of the channels. Left side: focused parts of the left hemisphere. Solid lines, major depressive disorder patients; dashed lines, healthy volunteers.

Dipole analysis. Under each condition and for each subject, equivalent current dipoles for P1m and MMNm were calculated separately for each hemisphere, utilizing a spherical head model constructed on the basis of an individual MRI and a subset of 54 channels over the temporal brain areas (Figure 3). ECD of P1m was calculated from standard stimuli for each condition. ECD of MMNm was calculated from the deviant-stimulus response wave minus the standard-stimulus response wave. ECDs of MMNm and P1m were calculated at the same latency determined by mGFP analysis. The ECDs with a goodness of fit (GOF) greater than 70% were included in the analysis. In this procedure, we reduced the number of channels to 32–49 when the dipole was not calculated or a certain channel had a considerable number of artifacts. The mean GOFs for P1m under the two conditions and in the two hemispheres ranged from 85.7% to 90.6% for the major depressive disorder patients and from 85.5% to 90.4% for the healthy volunteers. The mean GOFs for MMNm under the three conditions and in the two hemispheres ranged from 84.4% to 88.1% for the major depressive disorder patients and from 82.4% to 85.8% for the healthy volunteers. Whenever available, the ECD locations for each subject were superimposed on his/her 3D-reconstructed MRI. The *x*-axis defined the right and left directions, the *y*-axis defined the anterior and posterior directions, and the *z*-axis defined the superior and inferior directions.

Statistical Analyses

The reaction time and correct answer rate during the visual task performance, age, and sleepiness scores before and during the task performance were compared between groups by one-way analysis of variance (ANOVA). We excluded the data of the visual task performance (reaction time and correct answer rate) over 3 *SD*s lower or higher than the average. The mGFP peak latencies and powers of P1m and MMNm were analyzed using three-way ANOVA with group (major depressive disorder patients and healthy volunteer), condition (pure-tone frequency change condition, pure-tone duration change condition, and vowel across-category change condition) and hemisphere (left and right) as independent variables, followed by Scheffe's post hoc test where appropriate. Spearman's rho was calculated in exploratory analyses of the relationships among the visual task

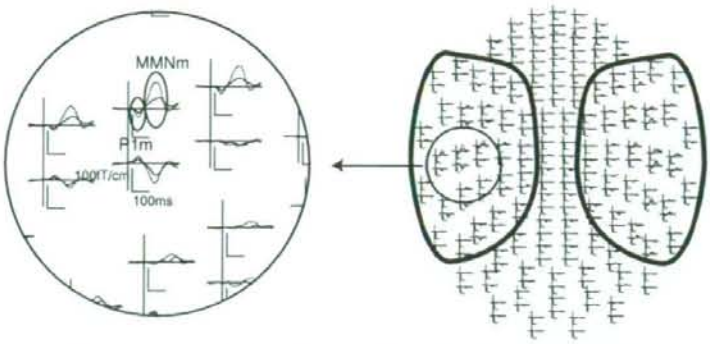

Figure 2. Formula for calculating mGFP. In this formula, n is the number of channels and u is the amplitude.

performance, clinical measures, and medications (reaction time, correct answer rate, age, HRSD score, age of onset, illness duration, and doses of antidepressants, anxiolytics, and hypnotics) and the mGFP power/peak latency or dipole location of P1m and MMNm.

The ECD locations of P1m and MMNm were compared between the two groups separately for each hemisphere using three-way ANOVA with group (major depressive disorder patients and healthy volunteer) and condition (pure-tone frequency change condition, pure-tone duration change condition, and vowel across-category change condition) as independent variables, followed by Scheffe's post hoc test where appropriate. The ECD location between P1m and MMNm was also compared separately for each hemisphere using one-way ANOVA. The statistical results were considered significant if $p<.05$ for the ANOVA of mGFP and the dipole analyses and $p<.01$ for the correlational analyses to avoid false positive findings in multiple correlation calculations.

Results

Behavioral Data

The reaction time during the visual task did not differ between the groups (major depressive disorder patients: mean, 588.3 ms; *SD*, 111.5; healthy volunteers: mean, 546.0 ms; *SD*, 70.6; $F[1,28] = 1.61$, $p = .22$). The correct answer rates in the visual task did not differ between the two groups (major depressive disorder patients: mean, 99.4%; *SD*, 0.5%; healthy volunteers: mean, 98.8%; *SD*, 1.3%). The Stanford sleepiness scores before and during the task did not significantly differ between the two groups.

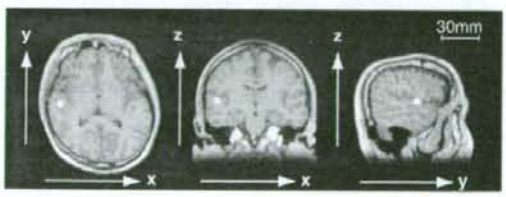

Figure 3. ECD location of MMNm of healthy volunteers for the pure-tone duration change condition in the left hemisphere. The arrows in this figure indicate each axis. The x-axis defines the right and left directions, the y-axis defines the anterior and posterior directions, and the z-axis defines the superior and inferior directions.

Magnetic Counterpart of Global Field Power (Table 2, Figures 4 and 5)

P1m. A three-way ANOVA of the mGFP power of P1m with group, condition, and hemisphere as independent variables revealed a significant effect of condition, $F(1,121) = 20.67$, $p<.01$, but not of group, hemisphere, or any interaction. A three-way ANOVA of the mGFP latency of P1m also revealed a significant effect of condition, $F(1,121) = 126.40$, $p<.01$, but not of group, hemisphere, or any interaction. Larger power and prolonged latency of mGFP in the vowel across-category change condition than in the pure tone condition were revealed.

MMNm. A three-way ANOVA of the mGFP power of MMNm with group, condition, and hemisphere as independent variables revealed significant effects of group, $F(1,186) = 7.01$, $p<.01$, and condition, $F(2,186) = 16.52$, $p<.01$, but not of hemisphere or any interaction. The mGFP powers of MMNm in the major depressive disorder patients were significantly smaller than those in the healthy volunteers. The Scheffe's post hoc test clarified that the mGFP powers of MMNm for pure-tone frequency change condition were significantly smaller than those for pure-tone duration change condition, $t(130) = 11.12$, $p<.01$, and vowel across-category change condition, $t(130) = 7.68$, $p<.01$. A post hoc two-way ANOVA of the mGFP power of MMNm with group and hemisphere as independent variables for each condition revealed trend-level significant effects of group in the vowel across-category condition, $F(1,62) = 3.04$, $p = .09$, and in the pure-tone duration change condition, $F(1,62) = 3.52$, $p = .07$, but not in the pure-tone frequency change condition, $F(1,62) = 0.61$, $p = .44$.

A three-way ANOVA of the mGFP latency of MMNm with group, condition, and hemisphere as the independent variables revealed a significant main effect of condition, $F(2,186) = 19.75$, $p<.01$, but not of group, hemisphere, or any interaction. The Scheffe's post hoc test clarified that the MMNm latencies were smaller in the pure-tone frequency change condition than in the pure-tone duration change condition, $t(135) = 30.46$, $p<.01$, and the vowel across-category change condition, $t(135) = 21.35$, $p<.01$.

Dipole Analysis

P1m. Reliable ECDs of P1m were successfully estimated in both the left and right hemispheres in 16 out of the 19 healthy

Table 2. *Three-Way Factorial ANOVA of mGFP Amplitudes of MMNm and P1m with Group, Condition, and Hemisphere*

		Group	Task	Hemisphere	Group × Task	Group × Hemisphere	Task × Hemisphere
MMNm	mGFP (fT/cm)	7.0**	16.5**	0.5	0.8	0.0	0.2
	mGFP latency (ms)	0.1	19.7**	0.3	1.8	1.2	0.2
P1m	mGFP (fT/cm)	2.2	20.7**	0.2	1.2	0.9	0.1
	mGFP latency (ms)	0.9	126.4**	3.5	0.1	1.0	0.0

Note: Group (major depressive disorder patients and healthy volunteers); Condition (vowel across-category change, pure-tone duration change, and frequency change); Hemisphere (right and left):
**$p < .01$.

subjects and in 12 out of 14 major depressive disorder patients and were estimated either in the left or the right hemisphere in 3 out of the 19 healthy subjects and in 3 out of the 14 major depressive disorder patients. A three-way ANOVA of x/mm, y/mm, and z/mm of estimated ECD locations with group, condition, and hemisphere as independent variables demonstrated a significant effect of hemisphere in y/mm, $F(1,118) = 31.93$, $p < .01$, and in z/mm, $F(1,118) = 13.13$, $p < .01$, but not of group, condition, or any interaction. These results indicate that the ECDs were located more anteriorly and superiorly in the left hemisphere than in the right hemisphere.

MMNm. Reliable ECDs of MMN1m were successfully estimated both in the left and right hemispheres in 15 out of the 19 healthy subjects and in 8 out of the 14 major depressive disorder patients, and were estimated either in the left or the right hemisphere in only 4 out of the 19 healthy subjects and in 6 out of the 14 major depressive disorder patients. A three-way ANOVA of x/mm, y/mm, and z/mm of estimated ECD locations with group, condition, and hemisphere demonstrated a main effect of condition in y/mm, $F(2,174) = 4.59$, $p = .01$, and hemisphere in y/mm, $F(1,174) = 26.69$, $p < .01$, but not of group or any interaction. The Scheffe's post hoc test clarified that the ECDs were located more anteriorly in the vowel across-category change condition than in the pure-tone duration change condition, $t(126) = 4.55$, $p = .02$, and also were located more anteriorly in the right hemisphere than in the left hemisphere.

Comparison between P1m and MMNm. A one-way ANOVA of x/mm, y/mm, and z/mm of estimated ECD locations with component (P1m and MMNm) in each hemisphere revealed a significant main effect of component in z/mm, $F(1,154) = 4.61$, $p = .03$: The MMNm dipole is located inferiorly to the P1m dipole in the left hemisphere.

Correlational Analysis

In the healthy volunteers, the MMNm power in the right hemisphere in the pure-tone duration change condition significantly correlated with age ($\rho = -0.64$, $p < .01$) and the reaction time ($\rho = 0.61$, $p < .01$). The MMNm duration in the left hemisphere in the pure-tone duration change condition significantly correlated with the reaction time ($\rho = -0.71$, $p < .01$). In the major depressive disorder patients, there was no significant correlation of P1m or MMNm power/latency with age, HRSD score, age of onset, reaction time, correct answer rate, or doses of antidepressants, anxiolytics, and hypnotics. The P1m latency in the left hemisphere under the pure-tone condition significantly correlated with illness duration ($\rho = 0.73$, $p < .01$).

Discussion

Summary of Results

In this study, we investigated MMNm and P1m responses in major depressive disorder patients and healthy volunteers. The results are summarized as follows: (1) mGFP of MMNm was significantly smaller in the major depressive disorder patients than in the healthy volunteers; (2) mGFP of P1m did not differ between the two groups; (3) mGFP of MMNm did not correlate with depressive symptoms, psychotropic medication, age of onset, or illness duration; and (4) the locations of the estimated MMNm and P1m dipoles did not significantly differ between the two groups. These results suggest impaired preattentive information processing in major depressive disorder patients irrespective of the depressive state and psychotropic medication.

Comparison with Previous Studies

As described in the introduction, there has been only one study of MMNm and P1m in major depressive disorder patients using MEG (Kähkönen et al., 2007), and there has been only one study that directly examined MMN in major depressive disorder patients using EEG (Umbricht et al., 2003). Kähkönen et al. found no significant differences in MMN amplitude or latency between major depressive disorder patients and healthy volunteers using pure-tone frequency deviant to elicit MMNm. Umbricht et al. (2003) found no significant differences in MMN amplitude or latency between major depressive disorder patients and healthy volunteers using pure-tone frequency deviant and pure-tone duration deviant to elicit MMNm. In our results, a three-way ANOVA of the mGFP power of MMNm with group, condition, and hemisphere as independent variables revealed significant effects of group, and a post hoc two-way ANOVA of the mGFP power of MMNm with group and hemisphere as independent variables for each condition revealed trend-level significant effects of group in the vowel across-category condition and in the pure-tone duration change condition but not in the pure-tone frequency change condition. This result is partly replicated in previous studies in the sense that the mGFP power and latency of MMNm were not significantly different between the major depressive disorder patients and the healthy volunteers in the pure-tone frequency change condition. However, our results were in disagreement with those of Umbricht et al. (2003) as well in the sense that the mGFP power of MMNm in the pure-tone duration change showed the trend-level significant effects in our study. There was a study showing that attention affects MMN power (Yucel, Petty, McCarthy, & Belger, 2005); thus, the difference in the methods of distracting the subjects' attention from the auditory stimuli may also be responsible for the difference between our results and Umbricht's results, because of the difference in the visual task procedure. However, an obvious difference between our study and their studies was in the physical